Journal of the Indian Institute of Science
Vol. 53, No 4, October 1971

SURFACE WAVE CHARACTERISTICS OF A CYLINDRICAL METALLIC CORRUGATED STRUCTURE EXCITED IN E_0-MODE*

(MISS) H M GIRIJA, AND S K. CHATTERJEE

[*Department of Electrical Communication Engineering, Indian Institute of Science, Bangalore-12, India*]

(Received: July 27, 1971)

ABSTRACT

The investigations are concerned with a systematic study of the electromagnetic surface wave characteristics of a cylindrical metallic conductor corrugated uniformly and excited in E_0-mode The investigations include

(i) *Determination of the parameters of the structure for which it can support a surface wave.*

(ii) *Study of the different properties of the surface wave such as*
   (a) *Guide wave length*
   (b) *Power flow*
   (c) *Dispersion characteristics*
   (d) *attenuation*
   and their variation with structure parameters.

(iii) *Study of the effect of higher order space harmonics on the propagation characteristics of the structure.*

1. INTRODUCTION

Since the work of Sommerfield[1,2], Zenneck[3], Harms[4], Hondros[5], Debye[6] and Weyl[7], considerable amount of work has been done on surface waves by Wait, Barlow, Brown, Cullen, Karbowiak, Schelkunoff, Chatterjee and others[8-39 and 46]. A thorough discussion on surface waves is given in an illuminating manner by Wait[15] in his paper "Electromagnetic surface waves". In the classification of different types of surface waves made by Wait, the common feature is that surface waves can be supported only by an interface

*The project is supported by PL-480, contract No. E-262-69 (N) August 1969.

between two different media. Barlow and Cullen's[16] definition of surface waves also emphasises that an interface between two different media or in other words, a physically recognisable surface is essential for supporting a surface wave.

Surface wave guides are essentially open wave guides in contrast to the conventional type of metallic guides with closed boundaries. The concept of modes excited in a conventional wave guide is well established. The question arises as to whether the same modal concept can be usefully employed in the case of surface wave guides, what type of modes can be supported by a surface wave guide in the absence of sources, their properties and what is their utility The answers to these questions are discussed by Marcuvitz, Schelkunoff, Goubau and others[17]. The difference between a closed conventional wave guide and a surface wave guide has been very clearly explained by Collin[18].

Since, in practice, launchers for the surface waves are restricted to a finite area, the surface wave problem is always associated with radiation. A complete solution to the surface wave problem requires the determination of source-excited fields. It has been shown by Zücker[19] that the total field on a surface wave guide can be synthesised by a superposition of all the modes excited by the source. The resulting field is then given by a contour integral, the integrand of which has poles and branch points in the plane of the complex propagation constant. The surface wave modes are associated with the residues at the poles. The branch points occur at the wave numbers in the two media on either side of the interface. By an appropriate deformation of the contour, the total integral can be split up into sum of residues at the poles plus one or two branch-cut integrals. The branch-cut integrals can be evaluated by means of the steepest descent method. The radiation field is associated with the evaluation of the branch-cut integral and represents the radiation field of the source modified by the presence of the structure.

The surface wave and the radiated field are merely different aspects of the same dynamic electromagnetic phenomenon. The sub-division is made for the sake of convenience of description. However, the separation of the surface wave field from the radiation field can only be visualised mathematically if the latter is properly defined. Goubau[21] has derived the following orthogonality relation between the surface wave and radiated fields using the reciprocity theorems

$$\int_S (\vec{E}_S \times \vec{H}_R) \cdot \vec{n} ds = \int_S (\vec{E}_R \times \vec{H}_S) \cdot \vec{n} ds = 0 \qquad [1]$$

where, the integration is carried over the equi-phase surface of the surface wave. The components $\vec{E}_R$, $\vec{H}_R$ and $\vec{E}_S$, $\vec{H}_S$ correspond to the radiated

and surface wave fields respectively. The above relation defines uniquely a radiation field which is not contaminated by the surface wave component.

For any electromagnetic structure to act as an efficient surface wave guide, it is necessary that the power contained in the radiation field be as small as possible. This requires that the efficiency of the launcher should be as high as possible. Collin[23] has given a complete and comprehensive treatment of surface wave excitation problems in his book "Field Theory of Guided waves". Wait[24] has made very significant contributions to the problem of source-exctied fields. Different types of surface wave launchers have been studied by Cullen[43], Brown and Stachera[44] and others[45-48] Three types of radiation fields (though these may not always exist independently of each other) may appear in any surface wave problem. These fields may be caused by (i) the radiation from the source in the presence of the guiding structure (when the efficiency of the launcher is poor), (ii) the radiation from the structure (when its length is finite), (iii) the presence of leaky waves on the structure (when the leaky wave poles exist). When the radiation field arises due to causes (ii) and (iii), the structure is referred to as a 'surface wave antenna' and a 'leaky wave antenna' respectively.

In the present investigation, the surface wave guide is composed of a cylindrical metallic corrugated rod which is a modified form of Harms-Goubau dielectric coated surface wave line. The dielectric coating is replaced by an artificial delay dielectric by loading a cylindrical metallic conductor uniformly with thin metallic discs. The main differences between this line and the Harms-Gaubau line are :

(i) The corrugated line is a periodic structure and hence the total field on the line has to be represented in terms of an infinite number of space harmonics, whereas the field on the Harms-Goubau surface wave line is represented in terms of a single mode and so the question of space harmonics does not arise.

(ii) In the case of corrugated line, the phase velocity and hence the field spread in the radial direction can be controlled by varying the two parameters of the structure, *viz.*, the disc-radius and disc-spacing. In the case of the Harms-Goubau line, the phase velocity is controlled by the thickness and dielectric constant of the dielectric coating.

The characteristics of corrugated and other periodic structures have been studied previously by several authors. A brief survey is given below.

Walkinshaw[25] has studied analytically the properties of a circular cylindrical wave guide having internal corrugation, with referrence to the dependence of phase velocity on frequency and wave guide dimensions. His work is concerned with the study of a linear accelerator for electrons.

Hurd[26] has studied the propagation characteristics of electromagnetic waves along an infinite corrugated surface by the method based on the calculus of residues, assuming that the slot walls are vanishingly thin. His study is mainly concerned with the phase velocity and 'mode amplitudes' of the surface waves.

Rotman[27] has made an experimental study of a flat grooved plate fed by a wave guide and also a corrugated cylindrical conductor fed by a co-axial line and has shown that such types of structures can support surface waves efficiently. He has also shown that the attenuation in such guides is chiefly due to ohmic losses in the metal rather than radiation.

Piefke[28] has shown in his study on the propagation characteristics of plane and cylindrical corrugated guides that these guides are similar to the Harms-Goubau guide if the depth of corrugation is small compared to the free space wave length. He has also shown that the attenuation and the phase velocity are functions of groove-depth. By increasing the groove-depth the field concentration around the structure can be increased. His treatment of the problem depends on considering the guide as a quasi-homogeneous, but anisotropic medium whose permitivity and permeability are complex.

Chu and Hansen[29] have studied theoretically the properties of an apertured disc-loaded wave guide and have derived relations for the phase velocity, group velocity, power flow, energy storage and losses.

Barlow and Karbowiak[30] have discussed the characteristics of the surface waves on corrugated cylindrical conductor and have concluded that a substantially pure surface wave mode can be supported by the structure. They have also shown that if the pitch of the groove is very much greater than the free space wave length, then the guiding property of the structure is completely destroyed.

Lines, Nicoll and Woodward[31] have discussed the characteristics of a periodically loaded wave guide using the concept of an equivalent transmission line analogy.

Harvey[32] has given an excellent and thorough review of the properties of periodic structures, including different types of slow-wave structures.

Wait[49] has given a unified treatment of surface waves which provides a link between the surface waves of Zenneck, Sommerfeld, Norton and Harms-Goubau. Cases of a metallic plane with a thin dielectric film and a corrugated surface are also discussed. This paper is considered to have made a significant contribution towards an understanding of surface waves in

that it has been able to develop a general connection between the various forms of seemingly unrelated surface waves. Wait[49] has treated the case of radiation from slots on dielectric clad and corrugated cylinders. Wait[24] has also discussed the excitation of surface waves in his treatment of " Guiding of electromagnetic waves by uniformly rough surfaces ".

From the information gathered from the available literature, it may be said that the work by previous authors on surface waves has made significant contribution to the subject of surface waves. However, it is felt that there is still much scope for the study of surface wave and radiation characteristics of corrugated structures. The study of electromagnetic structures with uniform corrugations has been undertaken with a view to gain knowledge and experience which can be utilised to investigate the characteristics of surface wave modulated structures which is the ultimate object of this project. It is believed that the results reported in this and in the succeeding two papers will make significant contributions to our existing knowledge on the characteristics of uniformly corrugated structures used as surface wave guide or surface wave antenna.

2. Theoretical Study of the Surface Wave Field

2.1. *Field Components* :

The structure (See Fig 1) consists of a solid conductor loaded uniformly with thin circular discs of the same material as that of the conductor. The discs are all of the same radius and the structure is periodic.

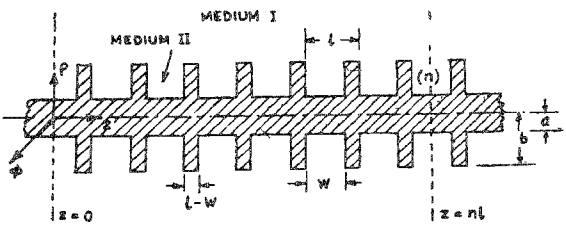

FIG. 1

Metal disc-loaded Sommerfeld surface wave line.

a : Radius of the inner rod
b : Disc Radius
t : Period of spacing
t-w : Thickness of the discs
(*n*) : No of the grove
w : Disc spacing
Medium I : Syace outside the structure
Medium II : Space within the grooves

To derive the expressions for the field components, the whole space is divided into two media I and II. Medium I ($\rho \geq b$) is the space outside the structure and medium II ($a \leq \rho \leq b$) is the space within the groove formed by any two adjacent metal discs and the surface of the inner conductor.

Medium I;

Since the structure is periodic of period l, according to Floquet's theorem, any field component say, E_z can be written as

$$E_z = f(\rho, z) \exp(-j\beta_0 z) \quad [2]$$

where, $f(\rho, z)$ is a periodic function of z of period l. Expanding $f(\rho, z)$ into its Fourier series, equation [2] becomes

$$E_z = \sum_{m=-\infty}^{\infty} C_m(\rho) \exp(-j\beta_m z) \quad [3]$$

where the functions $C_m(\rho)$ involve excitation constants and appropriate cylinder functions and are different for different values of m. The variable m takes integral values (including zero) from $-\infty$ to $+\infty$ The different values of m represent the orders of different space harmonics. The negative and positive values correspond respectively to backward and forward space harmonics. The one corresponding to $m=0$ is called the fundamental harmonic.

The quantities β_m represent the axial propagation constants of different space harmonics and are given by the relation

$$\beta_m = \beta_0 + (2\pi m/l) \quad [4]$$

where, $m=0, \pm1, \pm2, \pm3$, etc., and β_0 is the axial propagation constant of the fundamental harmonic ($m=0$).

The axial field component $E_z^{(1)}$ in medium I and the components $E_\rho^{(1)}$ and $H_\phi^{(1)}$ obtained from Maxwell's equations are as follows :

Medium I: $\rho \geq b$

$$E_z^{(1)} = \sum_{m=-\infty}^{\infty} C_m H_0^{(1)}(j\gamma_m \rho) \exp(-j\beta_m z)$$

$$E_\rho^{(1)} = \sum_{m=-\infty}^{\infty} C_m \frac{\beta_m}{\gamma_m} H_1^{(1)}(j\gamma_m \rho) \exp(-j\beta_m z)$$

$$H_\phi^{(1)} = \sum_{m=-\infty}^{\infty} C_m \frac{k_0^2}{\omega \mu_0 \gamma_m} H_1^{(1)}(j\gamma_m \rho) \exp(-j\beta_m z) \quad [5]$$

where, the axial propagation constant β_m is related to the propagation constant γ_m by the relation

$$\beta_m^2 = \gamma_m^2 + k_0^2 \qquad [6]$$

Medium II: $a \leq \rho \leq b$

Assuming that the spacing between the discs is small, each groove can be treated as a short-circuited radial transmission line. The dominant mode in such a transmission line is *T E M*. Thus the only field components that exist in medium II are E_z and H_ϕ. The field components in medium II can be written as

$$E_z^{(2)} = -[\mu_0 j\,\omega/k_0]\,[A_1 J_0(k_0\rho) + A_2 Y_0(k_0\rho)] \exp(-j\beta_0 nl)$$
$$H_\phi^{(2)} = [A_1 J_1(k_0\rho) + A_2 Y_1(k_0\rho)] \exp(-j\beta_0 nl) \qquad [7]$$

The phase term $\exp(j\beta_0 nl)$ is included to match the field components in media I and II. The integer n stands for the number of the groove counted from the plane $z=0$ (See Fig. 1) and A_1 and A_2 are amplitude constants. Applying the boundary condition that $E_z^{(2)}=0$ at $\rho=a$, the following relation between A_1 and A_2 is obtained from equation [7].

$$A_1/A_2 = -Y_0(k_0a)/J_0(k_0a) \qquad [8]$$

On substituting for A_1 in terms of A_2 in equation [7] and simplifying, it reduces to

$$E_z^{(2)} = A\,F_0(k_0\rho) \exp(-j\beta_0 nl)$$
$$H_\phi^{(2)} = jA\sqrt{(\mu_0/\epsilon_0)} \cdot F_1(k_0\rho) \exp(-j\beta_0 nl) \qquad [9]$$

where A is the excitation constant and

$$F_r(k_0\rho) = J_0(k_0a)\,Y_r(k_0\rho) - Y_0(k_0a)\,J_r(k_0\rho) \qquad [10]$$

where, the subscript $r=0,\ 1$.

2.2 *Variation of* E_z *over the mouth of the* n^{th} *groove*

The characteristic equation is easily formulated by matching the appropriate impedance at $\rho=b$, when it is assumed that the fundamental surface wave mode is predominant and the effect of the space harmonics is negligibly small. A more accurate equation can be derived by assuming a proper variation of E_z over the mouth of the groove.

The variation of E_z should be such that it not only satisfies the boundary conditions but also the singularity condition at the edges of the disc forming the grooves. The variation of E_z assumed below

$$E_z(\rho=b) = \frac{B \exp(-j\beta_0 nl)}{\sqrt{[1-(2z_n/W)^2]}} \qquad [11]$$

is found to satisfy the above conditions. B is the amplitude constant; the distance z_n is measured from the centre of the n^{th} groove and is given by

$$z_n = z - nl \qquad [12]$$

2.3 *Determination of the Amplitude constants* C_m *in terms of* B.

The amplitude constants C_m of the field components in medium I ($\rho \geq b$) are evaluated in terms of B by equating the expressions for E_z in equations [5] and [11] at $\rho = b$, *i.e.*

$$\sum_{m=-\infty}^{\infty} C_m H_0^{(1)}(j\gamma_m b) \exp(-j\beta_m z) = \begin{cases} \dfrac{B \exp(-j\beta_0 nl)}{\sqrt{[1-(2z_n/W)^2]}} & \text{for } |z_n| < W/2 \\ 0 & (W/2) \leq |z_n| \leq l/2 \end{cases} \qquad [13]$$

Multiplying both the sides of equation [13] by $\exp(j\beta_m z_n)$ and integrating with respect to z_n from $-l/2$ to $+l/2$, it becomes,

$$\int_{-l/2}^{+l/2} C_m H_0^{(1)}(j\gamma_m b) \exp[j\beta_m (z_n - z)]\, dz_n = B \int_{-W/2}^{W/2} \frac{\exp(j\beta_m z_n) \exp(-j\beta_0 nl)}{\sqrt{[1-(2z_n/W)^2]}}\, dz_n \qquad [14]$$

On substituting for z_n from equation [12] and simplifying, equation [14] becomes

$$l \cdot C_m H_0^{(1)}(j\gamma_m b) = B \int_{-W/2}^{+W/2} \frac{\exp(j\beta_m z_n)}{\sqrt{[1-(2z_n/W)^2]}}\, dz_n \qquad [15]$$

The integral on the right hand side of equation [15] is equal to $(\pi W/2) \times J_0[\beta_m (W/2)]$.

Therefore, from equation [15] the constant C_m is given by the equation

$$C_m = \frac{\pi W B}{2l} \cdot \frac{J_0(\beta_m W/2)}{H_0^{(1)}(j\gamma_m b)} \qquad [16]$$

2.4 *Determination of the amplitude constant* A *in terms of* B.

To evaluate the amplitude constant A of the fields in medium II ($a \leq \rho \leq b$) in terms of B, the axial component of the electric field in

medium II is matched with the average value of the axial component of the electric field in medium I over the mouth of the n^{th} groove, *i.e.*

$$E_z^{(2)} = E_z^{(1)} \text{ (average) at } \rho = b \qquad [17]$$

$$E_z^{(1)} \text{ (average)} = (B/W) \int_{-W/2}^{+W/2} \frac{\exp(-j\beta_0 nl)}{\sqrt{[1-(2z_n/W)^2]}}\, dz_n \qquad [18]$$

at $(\rho = b)$

$$E_z^{(2)} = A F_0(k_0 b) \exp(-j\beta_0 nl) \qquad [19]$$

at $(\rho = b)$

where,

$$F_0(k_0 b) = J_0(k_0 a)\, Y_0(k_0 b) - Y_0(k_0 a)\, J_0(k_0 b) \qquad [20]$$

Equating the expressions on the right hand sides of equations [18] and [19] and integrating, the following expression is obtained for the amplitude constant A.

$$A = (\pi B/2)\,[F_0(k_0 b)]^{-1} \qquad [21]$$

where, $F_0(k_0 b)$ is given by equation [20]

2.5 *Derivation of the characteristic Equation*

The characteristic equation is derived by matching the average value of the azimuthal component of the magnetic field in medium I ($H_\phi^{(1)}$) with the azimuthal component of the magnetic field in medium II ($H_\phi^{(2)}$) over the mouth of the n^{th} groove, *i.e.*,

$$H_\phi^{(1)} \text{ (average)} = H_\phi^{(2)} \text{ at } \rho = b \qquad [22]$$

The average value of $H_\phi^{(1)}$ at $\rho = b$ is

$$H_\phi^{(1)} \text{ (average) at } \rho = b$$

$$= (1/W) \sum_{m=-\infty}^{\infty} C_m \frac{k_0^2}{\omega \mu_0 \gamma_m} H_1^{(1)}(j\gamma_m b) \int_{-W/2}^{W/2} \exp(-j\beta_m z)\, dz \qquad [23]$$

and,

$$H_\phi^{(2)} \text{ (at } \rho = b) = A j \sqrt{(\epsilon_0/\mu_0)} \cdot F_1(k_0 b) \exp(-j\beta_0 nl) \qquad [24]$$

where,

$$F_1(k_0 b) = J_0(k_0 a)\, Y_1(k_0 b) - Y_0(k_0 a)\, J_1(k_0 b) \qquad [25]$$

Using equations [25] and [24] in equation [22], it becomes,

$$\sum_{m=-\infty}^{\infty} C_m \frac{k_0^2}{\omega \mu_0 \gamma_m} H_1^{(1)}(j\gamma_m b)(1/W) \frac{2\sin[\beta_m W/2]}{\beta_m} = A J\sqrt{(\epsilon_0/\mu_0)} \cdot F_1(k_0 b) \quad [26]$$

Substituting for A and C_m from equations [21] and [16] respectively in equation [26], it becomes,

$$\frac{2k_0}{l} \sum_{m=-\infty}^{\infty} \frac{J_0(\beta_m W/2)\sin(\beta_m W/2)}{\beta_m \gamma_m} \frac{H_1^{(1)}(j\gamma_m b)}{H_0^{(1)}(j\gamma_m b)} = j \frac{F_1(k_0 b)}{F_0(k_0 b)} \quad [27]$$

Or, writing $H_0^{(1)}(j\gamma_m b)$ and $H_1^{(1)}(j\gamma_m b)$ in terms of modified Bessel functions $K_0(\gamma_m b)$ and using the relations,

$$H_0^{(1)}(j\gamma_m b) = -j K_0(\gamma_m b)\, 2/\pi \quad [28]$$

$$H_1^{(1)}(j\gamma_m b) = -K_1(\gamma_m b)\, 2/\pi \quad [29]$$

equation [27] becomes,

$$\sum_{m=-\infty}^{\infty} \frac{2k_0}{l} \cdot \frac{J_0(\beta_m W/2)\sin(\beta_m W/2)}{\beta_m \gamma_m} \frac{K_1(\gamma_m b)}{K_0(\gamma_m b)} = -\frac{F_1(k_0 b)}{F_0(k_0 b)} \quad [30]$$

where, $F_0(k_0 b)$ and $F_1(k_0 b)$ are given by equations [20] and [25].

2.6 *Solution of the Characteristic Equation*

Since $\beta_m = \beta_0 + (2\pi m/l)$ and $\gamma_m = \sqrt{(\beta_m^2 - k_0^2)}$

the solution of equation [30] for the determination of the propagation constant reduces to the problem of determining β_0, the axial propagation constant for the fundamental harmonic. The arguments $\beta_m W/2$ and $\gamma_m b$ of the Bessel functions may vary over a wide range and approximations cannot be readily made for the Bessel functions. The expression on the left hand side of equation [30] can be simplified by assuming that only the fundamental harmonic ($m = 0$) is present. This equation then is simplified to

$$\frac{2k_0}{l} \frac{J_0(\beta_0 W/2)\sin(\beta_0 W/2)}{\beta_0} = -\gamma_0 \frac{K_0(\gamma_0 b)}{K_1(\gamma_0 b)} \cdot \frac{F_1(k_0 b)}{F_0(k_0 b)} \quad [31]$$

which is of the form $f(\beta_0) = g(\beta_0)$, where

$$f(\beta_0) = \frac{2k_0}{l} \cdot \frac{J_0(\beta_0 W/2)\sin(\beta_0 W/2)}{\beta_0} \quad [32]$$

$$g(\beta_0) = -\gamma_0 \frac{K_0(\gamma_0 b)}{K_1(\gamma_0 b)} \cdot \frac{F_1(k_0 b)}{F_0(k_0 b)} \qquad [33]$$

When β_0 and γ_0 are both real, $f(\beta_0)$ and $g(\beta_0)$ are real and continuous and equation [31] can be readily solved by numerical methods. An approximate range for β_0 is first of all determined by computing $f(\beta_0) - g(\beta_0)$ over a suitable range of values of β_0 The accurate root is then determined by the successive bisection method.

2.7 *Surface wave Roots of the Characteristic Equation*

Assuming the structure to be losseless, it can act as a surface wave guide if the roots β_0 and γ_0 are both real For given values of disc radius (b) and disc-spacing (W) whether equation [31] has a surface wave root or not depends on whether the curves $f(\beta_0)$ *Vs* β_0 and $g(\beta_0)$ *Vs* β_0 intersect at a real point or not. Since $f(\beta_0)$ and $g(\beta_0)$ are both even functions of β_0, it is sufficient to consider either positive or negative values of β_0 If β_0 is a root of equation [31], then $-\beta_0$ is also a root of this equation. The positive values of β_0 give rise to waves travelling in the positive z-direction. Hence only positive values of β_0 have been considered.

2.8 *Variation of $f(\beta_0)$, $g(\beta_0)$ and $F_1(k_0 b)/F_0(k_0 b)$ with respect to their arguments.*

The study of the nature of different functions involved in the characteristic equation helps in a proper understanding of the conditions of existence of surface wave roots.

2.8.1 *Properties of $f(\beta_0)$:*

(i) $f(\beta_0)$ is an oscillatory function of β_0 with decreasing amplitude.

(ii) $|f(\beta_0)| \to 0$ as $\beta_0 \to \infty$.

(iii) $f(\beta_0)$ depends on W but is independent of b.

2.8.2 *Properties of $g(\beta_0)$:*

(i) $g(\beta_0)$ does not change its sign when β_0 is varied.

(ii) $|g(\beta_0)|$ is an increasing function of β_0

(iii) $|g(\beta_0)| \to \infty$ as $\beta_0 \to \infty$.

(iv) $g(\beta_0)$ depends on b but is independent of W.

(v) $g(k_0) = 0$.

2.8.3 *Properties of* $F_1(k_0b)/F_0(k_0b)$:

(i) $F_1(k_0b)/F_1(k_0b)$ varies from $-\infty$ to $+\infty$ when b is varied over positive values.

(ii) $F_1(k_0b)/F_0(k_0b)$ has poles and zeros at the roots of $F_0(k_0b)=0$ and $F_1(k_0b)=0$ respectively.

(iii) $F_1(k_0b)/F_0(k_0b)$ is discontinuous when $F_0(k_0b)=0$.

It is to be noted that for any value of b, the sign of $g(\beta_0)$ is positive or negative according as $F_1(k_0b)/F_0(k_0b)$ is negative or positive.

2.9 *Condition for the Existence of Surface Wave Roots.*

The condition of the existence of surface wave roots can be determined from the properties of the functions discussed in Section 2.8.

Since $f(\beta_0)$ oscillates and decreases to zero and $|g(\beta_0)|$ increases to infinity as β_0 tends to infinity, it follows that surface wave roots exist when

(i) $f(k_0)$ and $g(\beta_0)$ are of the same sign For if $f(k_0)>0$ and $g(\beta_0)>0$ [note that $g(\beta_0)$ does not change its sign when β_0 is varied and $g(k_0)=0$], then $f(k_0)>g(k_0)$ and there exists a value β' such that $f(\beta')<g(\beta')$. Hence, the curves $f(\beta_0)$ versus and $g(\beta_0)$ versus β_0 intersect at a point in the interval (k_0, β').

(ii) $f(k_0)$ and $g(\beta_0)$ are of opposite signs and $|f(\beta'')|>|g(\beta'')|$, where $f(\beta'')$ is the first minimum value of $f(\beta_0)$, when $f(k_0)>0$ and its first maximum value when $f(k_0)<0$. For, if $f(k_0)>0$ and $g(\beta_0)<0$, then $f(k_0)>g(k_0)$ and $f(\beta'')<g(\beta'')$ Hence, the curves $f(\beta_0)$ versus β_0 intersect at a point in the interval (k_0, β'').

2.10 *Classification of Structure Parameters*:

The surface wave roots of the characteristic equation [31] exist only if the functions $f(\beta_0)$ and $g(\beta_0)$ satisfy definite conditions (See section 2.9). Otherwise, such a root does not exist Thus the structure parameters b and W can be grouped into two classes. Class I consists of combinations of b and W (relative to the radius of the inner rod, a) for which a surface wave root exists and class II consists of all combinations of b and W for which a surface wave root does not exist.

It follows from the discussion in section 2.9, that all combinations of b and W satisfying the following conditions (i) and (ii) belong to class I.

(i) $F_1(k_0b)/F_0(k_0b)$ and $f(k_0)$ are of opposite signs. (in this case $f(k_0)$ and $g(\beta_0)$ are of the same sign).

(ii) $F_1(k_0b)/F_0(k_0b)$ and $f(k_0)$ are of the same sign and $|f(\beta'')| > |g(\beta'')|$, where $f(\beta'')$ is the first minimum value of $f(\beta_0)$ when $f(k_0) > 0$ and its first maximum value when $f(k_0) < 0$ (In this case $f(k_0)$ and $g(\beta_0)$ will be of opposite signs).

The combinations of b and W belonging to class II are such that $F_1(k_0b)/F_0(k_0b)$ and $f(k_0)$ are of the same sign and $|f(\beta'')| < |g(\beta'')|$. ($\beta''$ being the same as that defined in the previous paragraph).

It is to be noted that the existence of only the TEM mode in the grooves requires $W \leq \lambda_0/2$. When $W \leq \lambda_0/2$, $f(k_0) < 0$. It can be seen that in this case, the classification of structure parameters can be effected referring to only the values of b. The condition for the existence of surface wave roots can be restated as follows. All combinations of b and W such that

(i) $F_1(k_0b)/F_0(k_0b) < 0$.

(ii) $F_1(k_0b)/F_0(k_0b) > 0$ and $|f(\beta'')| > |g(\beta'')|$ where $f(\beta'')$ is the first minimum value of $f(\beta_0)$ and $W \leq \lambda_0/2$ belong to class I. It is obvious that $|f(\beta'')| > |g(\beta'')|$ implies that $F_1(k_0b)/F_0(k_0b)$ is small.

Plots of $f(\beta_0)$ and $g(\beta_0)$ *Vs* β_0 are given in Figures 2 and 3 for typical values of b and W. In Fig. 2, $g(\beta_0) > 0$ and hence the curves intersect at a real point. In Fig. 3, $g(\beta_0) < 0$ and hence the curves do not intersect at a real point.

2.11 *Discussion of the root* β_0 *as a function of* b *and* W :

Since $\gamma_0 = \sqrt{(\beta_0^2 - k_0^2)}$, γ_0 is real when $\beta_0 \geq k_0$ That is the phase velocity v_p of the wave is less than the free space wave velocity c and the guide wave length λ_g is less than the free space wavelength λ_0. For $\beta_0 = k_0$, $v_p = 0$. $\beta_0 < k_0$, $v_p = 0$. For $\beta_0 < k_0$, $v_p > c$. γ_0 is imaginary and the surface wave character is no longer maintained Hence the structure parameters corresponding to $\beta_0 = k_0$ or $v_p = 0$ may be considered to represent a transition stage from class I to class II.

When $v_p = 0$, the phase constant β_0 may be said to be matched to the free space wave number, which is the condition for the existence of a radiated wave.

The plot of β_0 versus the disc radius b for a fixed value of the disc-spacing W consists of a set of discrete curves. The different ranges of b in which the curves are defined belong to class I. The allowed range of values of when b and W belong to class I is from k_0 to ∞.

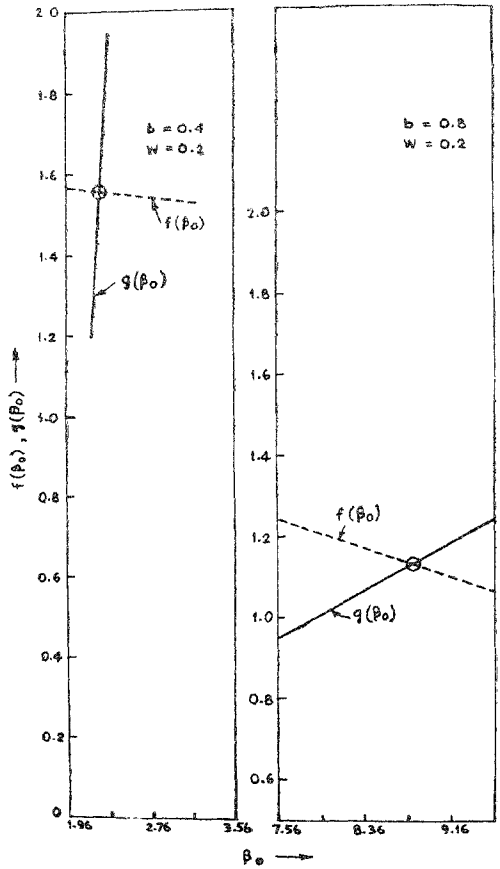

FIG. 2

Plots of $f(\beta_0)$, $g(\beta_0)$ verses β_0 for values of b and w belonging to class I
b: Disc-radius in cm; w: Disc-spacing in cm.
(All the values are approximated to two places).

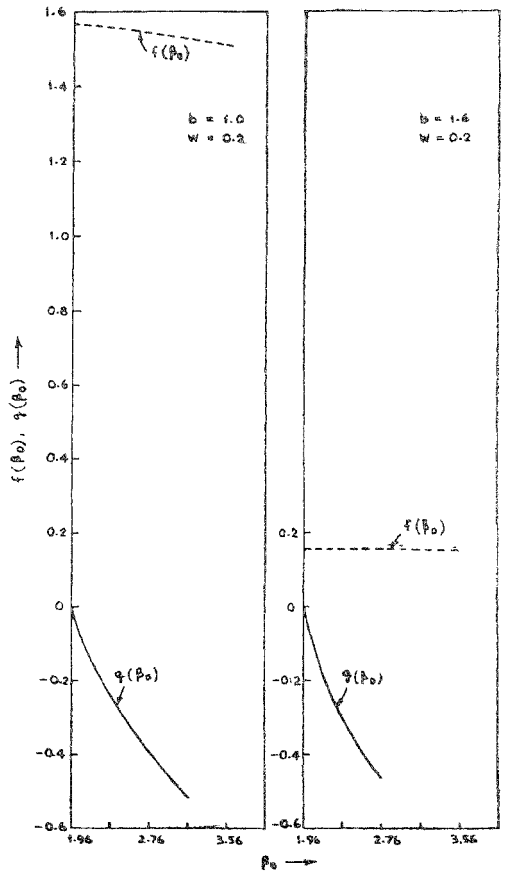

FIG. 3

Plots of $f(\beta_0)$, $g(\beta_0)$ versus β_0 for values of b and W belonging to class II
b : Disc-radius in cm ; W: Disc-spacing in cm.
(All the values are approximated to two places)

It can be shown that the extreme values of β_0 in class I correspond to the values of b satisfying the equations $F_0(k_0 b) = 0$ and $F_1(k_0 b) = 0$. These two cases are considered in the following sections.

2.11.1 *Root β_0 when $F_0(k_0 b) = 0$*

The characteristic equation [31] can be written in the form,

$$\frac{l}{2k_0} \cdot \frac{\beta_0 \gamma_0}{J_0(\beta_0 W/2) \sin(\beta_0 W/2)} \cdot \frac{K_0(\gamma_0 b)}{K_1(\gamma_0 b)} \cdot = -\frac{F_0(k_0 b)}{F_1(k_0 b)} \qquad [34]$$

when $F_0(k_0 b) = 0$, equation [34] becomes,

$$\frac{l}{2k_0} \cdot \frac{K_0(\gamma_0 b)}{K_1(\gamma_0 b)} \cdot \frac{\beta_0 \gamma_0}{J_0(\beta_0 W/2) \sin(\beta_0 W/2)} = 0 \qquad [35]$$

It can be shown that $\beta_0 = k_0$ is a root of this equation. For when $\beta_0 = k_0$, $\gamma = 0$ and the modified Bessel functions can be replaced by their respective small argument approximations as follows :

$$K_0(\gamma_0 b) \approx -(2/\pi) \ln(0{\cdot}89\ \gamma_0 b)$$

$$K_1(\gamma_0 b) \approx 2/(\pi\ \gamma_0 b) \qquad [36]$$

Substituting for $K_0(\gamma_0 b)$ and $K_1(\gamma_0 b)$ in equation [36], the following equation is obtained*.

$$\gamma_0^2 \ln(0.89\ \gamma_0 b) = 0 \qquad [37]$$

$\gamma_0 = 0$ is a root of this equation.

2.11.2 *Root β_0 when $F_1(k_0 b) = 0$. When $F_1(k_0 b) = 0$ the characteristic eq.* [31] *becomes* :

$$\frac{2k_0}{l} \cdot \frac{J_0(\beta_0 W/2) \sin(\beta_0 W/2)}{\beta_0 \gamma_0} \cdot \frac{K_1(\gamma_0 b)}{K_0(\gamma_0 b)} = 0 \qquad [38]$$

This equation has the roots β_0, given by

$$\sin(\beta_0 W/2) = 0 \qquad [39]$$

$$J_0(\beta_0 W/2) = 0 \qquad [40]$$

$$\beta_0 = \infty \qquad [41]$$

*It can be assumed that $J_0(k_0 W/2) \neq 0$ and $\sin(k_0 W/2) \neq 0$ For the values of W that makes $J_0(k_0 W/2) = 0$ or $\sin(k_0 W/2) = 0$ exceeds $\lambda_0/2$, but the existence of the TEM mode in the grooves requires $W \leqslant \lambda_0/2$.

Thus it is proved that the allowed range of β_0 is from k_0 to ∞. The significance of equations [39] and [40] is discussed later. (see section 18)

2.12 *Field components for the Fundamental Harmonic*

When the structure supports only the fundamental harmonic the field components of the surface wave are given by

$$E_z^{(1)} = C_0 H_0^{(1)} (j \gamma_0 \rho) \exp(-j \beta_0 z)$$

$$E_\rho^{(1)} = C_0 (\beta_0 / \gamma_0) H_1^{(1)} (j \gamma_0 \rho) \exp(-j \beta_0 z)$$

$$H_\phi^{(1)} = C_0 [k_0^2 / (\omega \mu_0 \gamma_0)] H_1^{(1)} (j \gamma_0 \rho) \exp(-j \beta_0 z) \qquad [42]$$

The radial propagation constant λ_0 determines the extent to which the field spreads in the radial direction. The amplitude of E_z decays radially as $|H_0^{(1)} (j \gamma_0 \rho)|$ and those of E_ρ and H_ϕ decay as $|H_1^{(1)} (j \gamma_0 \rho)|$. Thus the rate of decay in the radial direction increases as γ_0 increases.

Maximum and minimum field spread occur for values of b satisfying the equations $F_0 (k_0 b) = 0$ and $F_1 (k_0 b) = 0$ respectively. In the former case $\gamma_0 = 0$ and in the latter case $\gamma_0 = \infty$. These two cases represent the limiting cases in Class I.

2.13 *Phase Velocity and Guide Wavelength for the Fundamental Harmonic*

For a given value of k_0 (or λ_0), the values of phase velocity $v_p (= \omega / \beta_0)$ and guide wavelength $\lambda_g (= 2\pi / \beta_0)$ depend on b and W. The minimum values of λ_g and v_p are $\lambda_g = 0$ and $v_p = 0$ respectively. These values of v_p and λ_g correspond to the value of b satisfying the equation $F_1 (k_0 b) = 0$. The maximum values of λ_g and v_p given by $\lambda_g = \lambda_0$ and $v_p = e$ correspond to the value of b satisfying $F_0 (k_0 b) = 0$. It may be noted that $v_p = 0$ gives the condition for the existence of a radiated wave and implies that there is no propagation in the axial direction.

2.14 *Dispersion Characteristics of the Structure for the Fundamental Harmonic.*

The effect of frequency variation on the propagation characteristics of the structure can be studied from the roots of the characteristic equation [31] The surface wave roots exist only for definite ranges of k_0. The dispersion diagrams (β_0 *Vs* k_0) consist of a discrete set of curves, each defined in the interval (pass band) of k_0 in which a surface wave root exists. Any two such consecutive intervals are separated by an interval are separated by an interval (stop band) of k_0 in which a surface wave root does not exist. The

ranges of k_0 (for fixed values of b and W) in the pass and stop bands are defined as follows:

(*a*) *Pass-band*:

k_0 belongs to the pass band when

(i) $f(k_0)$ and $F_1(k_0 b)/F_0(k_0 b)$ are of opposite signs and

(ii) $f(k_0)$ and $F_1(k_0 b)/F_0(k_0 b)$ are of the same sign and $|f(\beta'')| > |g(\beta'')|$, where $f(\beta'')$ is the first minimum value of $f(\beta_0)$

(*b*) *Stop-band*:

k_0 belongs to the stop band when $f(k_0)$ and $F_1(k_0 b)/F_0(k_0 b)$ are of the same sign and $|f(\beta'')| < |g(\beta'')|$.

2.15 *Roots of the Characteristic Equation in the pass-band.*

The allowed range of β_0 (see Section 2.11) in the pass-band is from $\beta_0 = k_0$ to $\beta_0 = \infty$. These two values of β_0 correspond to values of k_0 satisfying the equation $F_0(k_0 b) = 0$ and $F_1(k_0 b) = 0$ respectively.

2.16 *Effect of Higher Order Space Harmonics.*

The characteristic equation [30] can be written in the form

$$\sum_{m=-\infty}^{+\infty} \bar{f}(\beta_m) = -\frac{F_1(k_0 b)}{F_0(k_0 b)} \qquad [43]$$

where,

$$\bar{f}(\beta_m) = \frac{2 k_0}{l} \frac{J_0(\beta_m W/2) \sin(\beta_m W/2)}{\beta_m \gamma_m} \frac{K_1(\gamma_m b)}{K_0(\gamma_m b)} \qquad [44]$$

The nature of the equation [43] is discussed below.

2.16 *Inequalities for the function* $\bar{f}(\beta_m)$.

Numerical computation of the functions $\bar{f}(\beta_m)$ shows that when $W \leq \lambda_0/2$, $|\bar{f}(\beta_m)| >> |\bar{f}(\beta_n)|$ for $|\beta_m| < |\beta_n|$. Since $\bar{f}(\beta_m)$ is an even function of β_m, it follows that whatever is true of $\bar{f}(\beta_m)$ for $\beta_0 < 0$ and $m \gtrless 0$ is true for $\beta_0 > 0$ and $m \lesseqgtr 0$ also. Thus it is sufficient to study the characteristic equation either for $\beta_0 > 0$ and $m \gtrless 0$ or $\beta_0 < 0$ and $m \gtrless 0$. In the present case, the former condition is assumed.

It follows from the above inequality for $\bar{f}(\beta_m)$ that the terms of the series in equation [43] corresponding to $m > 0$ can be neglected compared to that corresponding to $m = 0$

The relative magnitudes of β_m in different ranges of β_0 are given in Table 1 and are summerised in Fig. 4 For $\beta_0 = \beta'_m$, where $(2\pi m/l) = k_0 < \beta'_m < (2\pi m/l) + k_0$ $(m > 0)$. γ_{-m} is imaginary. Since the discussion is restricted to only real values of $\bar{f}(\beta)$, the values β'_m are not considered in the table. It is seen from table 1 that if a quantity $\beta_0 = d$ belongs to range (0), then $(2\pi m/l) - d$ $(m > 0)$ belongs to range m and $(2\pi m/l) + d$ belongs to m^1. Similarly, if $\beta_0 = d$ belongs to range (0, 1), then $2\pi m/l + d$ belongs to the range $(m, m+1)$. The following inequalities for $\bar{f}(\beta_m)$ follow as a consequence of the inequalities for β_m given in Table 1.

$$|\bar{f}(\beta_0)| >> |\bar{f}(\beta_m)|, \quad m \neq 0 \quad \text{in the range (0)}$$

$$|\bar{f}(\beta_{-1})| >> |\bar{f}(\beta_m)|, \quad m \neq -1 \text{ in the range (1), } (1)^1$$

$$|\bar{f}(\beta_{-2})| >> |\bar{f}(\beta_m)|, \quad m \neq -2 \text{ In the range (2), } (2)^1.$$

and

$$|\bar{f}(\beta_0)| \approx |\bar{f}\beta_{-1})| >> |\bar{f}(\beta_m)|, \quad m \pm 0, \ -1 \text{ in the range } (0, 1)$$

$$|\bar{f}(\beta_{-1})| \approx |\bar{f}(\beta_{-2})| >> |\bar{f}(\beta_m)|, \quad m \pm -1, \ -2 \text{ in the range } (1, 2), \text{ etc.}$$

The characteristic equation [30] can be simplified using the above inequalities.

2 16.2 *Simplification of the characteristic Equation.*

It follows from the above inequalities for $\bar{f}(\beta_m)$ that the infinite series on the left hand side of equation [43] can be approximated to the following sets of equations defined in different ranges of β_0

Set 1 :

(i) $\bar{f}(\beta_0) = -[F_1(k_0b)/F_0(k_0b)]$ in the range (0)

(ii) $\bar{f}(\beta_{-1}) = -[F_1(k_0b)/F_0(k_0b)]$ in the ranges (1), $(1)^1$

(iii) $\bar{f}(\beta_{-2}) = -[F_1(k_0b)/F_0(k_0b)]$, in the ranges (2), $(2)^1$, etc. [45]

Set II :

(i) $\bar{f}(\beta_0) + \bar{f}(\beta_{-1}) \simeq 2\bar{f}(\beta_0) = -[F_1(k_0b)/F_0(k_0b)]$ in the range (0, 1)

(ii) $\bar{f}(\beta_{-1}) + \bar{f}(\beta_{-2}) \approx 2\bar{f}(\beta_{-1}) = -[F_1(k_0b)/F_0(k_0b)]$ in the range (1.2), etc. [46]

TABLE I

Relative magnitudes of β_{-m} in different ranges of β_0

No.	Range β_0	Relative magnitudes of β_m
(0)	$k_0 < \beta_0 < \pi/l$	$\lvert\beta_0\rvert < \lvert\beta_m\rvert$, $m \neq 0$; $\beta_{-m} < 0$ for $m > 0$
(0.1)	$\lvert\beta_{-1}\rvert \approx (\pi/l)$	$\lvert\beta_0\rvert \approx \lvert\beta_{-1}\rvert$; $\lvert\beta_0\rvert$, $\lvert\beta_{-1}\rvert < \lvert\beta_m\rvert$
(1)	$(\pi/l) < \beta_0 < (2\pi/l) - k_0$	$\lvert\beta_{-1}\rvert < \lvert\beta_m\rvert$, $m \neq -1$; $\beta_{-m} < 0$ for $\lvert m\rvert > 0$
(1)^1	$(2\pi/l) + k_0 < \beta_0 < (3\pi/l)$	$\lvert\beta_{-1}\rvert < \lvert\beta_m\rvert$, $m \neq -1$; $\beta_{-m} < 0$ for $m > 1$
(1.2)	$\lvert\beta_0\rvert \approx (3\pi/l)$	$\lvert\beta_{-1}\rvert \approx \lvert\beta_{-2}\rvert$; $\lvert\beta_{-1}\rvert$, $\lvert\beta_{-2}\rvert < \lvert\beta_m\rvert$ for $m \neq -1, -2$
(2)	$(3\pi/l) < \beta_0 < (4\pi/l) - k_0$	$\lvert\beta_{-2}\rvert < \lvert\beta_m\rvert$, $m \neq -2$; $\beta_{-m} < 0$ for $\lvert m\rvert > 1$
(2)^1	$(4\pi/l) + k_0 < \beta_0 < (5\pi/l)$	$\lvert\beta_{-2}\rvert < \lvert\beta_m\rvert$, $m \neq -2$; $\beta_{-m} < 0$ for $\lvert m\rvert > 2$
(n)	$[(2n-1)\pi/l] < \beta_0 < (2n\pi/l) - k_0$	$\lvert\beta_{-n}\rvert < \lvert\beta_m\rvert$, $m \neq -n$; $\beta_{-m} < 0$ for $\lvert m\rvert > n-1$
$(n)^1$	$(2n\pi/l) + k_0 < \beta_0 < [(2n+1)\pi/l]$	$\lvert\beta_{-n}\rvert < \lvert\beta_m\rvert$, $m \neq -n$, $\beta_{-m} < 0$ for $\lvert m\rvert > n$
$(n+1)$	$\lvert\beta_0\rvert \approx [(2n+1)\pi/l$	$\lvert\beta_{-n}\rvert \approx \lvert\beta_{-(n+1)}\rvert$; $\lvert\beta_{-n}\rvert$, $\lvert\beta_{-(n+1)}\rvert < \lvert\beta_m\rvert$ for $m \neq -n, -(n+1)$

It can be seen from equations [45] and [46] that if $\beta_0 = d$ is a root of the first equation of the set I, then $\beta_0 = 2\pi m/l \pm d$ $(m > 0)$ is a root of the $(m+1)^{th}$ equation of the same set. For,

$$\bar{f}(\beta_{-m}) = \bar{f}[\beta_0 - (2\pi m/l)]$$

if $\beta_0 = (2\pi m/l) \pm d$, then

$$\bar{f}(\beta_{-m}) = \bar{f}(\pm d) = \bar{f}(d)$$

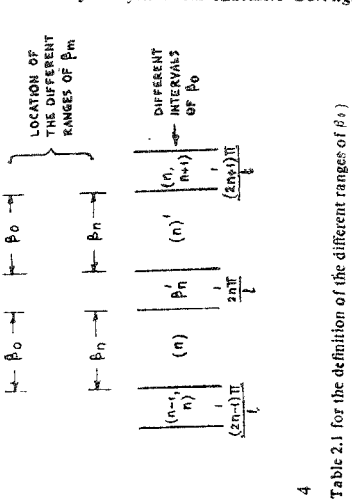

FIG. 4

Relative magnitudes of β_m in different ranges of β_0. (See Table 2.1 for the definition of the different ranges of β_0.)

and therefore, if $\beta_0 = d$ is a root of the first equation of the set I, then $\beta_0 = (2\pi m/l) \pm d$ is a root of the $(m+1)^{th}$ equation of the same set. Similarly, if $\beta_0 = d$ is a root of the first equation of the set II, then $(2\pi m/l) \pm d$ are respectively the roots of $(m+1)^{th}$ and $(m+2)^{th}$ equations of the same set. That is the roots of different equations of a set can be derived from any one equation of the same set. Thus when the existence of space harmonics cannot be ignored, the following equations have to be solved for

$$\bar{f}(\beta_0) = -[F_1(k_0 b)/F_0(k_0 b)] \qquad [47]$$

where, β_0 belongs to the range (0) and

$$2\bar{f}(\beta_0) = -F_1(k_0 b)/F_0(k_0 b) \qquad [48]$$

where, β_0 belongs to the range (0, 1). The roots of the characteristic equation [43] are then given by the values $(2\pi m/l) \pm \beta_0$, $(m > 0)$. Eq. [47] and [48] can be written in the form

$$f_1(\beta_0) = -[F_1(k_0 b)/F_0(k_0 b)]. \qquad [49]$$

where,

$f_1(\beta_0) = 2\bar{f}(\beta_0)$ for (β_0) in the range (0) [50]

$f_1(\beta_0) = 2\bar{f}(\beta_0)$ for (β_0) in the range (0, 1) [51]

2.17 *Relative Amplitudes of Harmonics*:

At any point, the ratio of the amplitudes A_m and A_n of the component E_z of the m^{th} and n^{th} space harmonics, respectively is given by

$$\frac{A_m}{A_n} = \left|\frac{J_0(\beta_m W/2)}{J_0(\beta_n W/2)}\right| \cdot \frac{K_0(\gamma_n b)}{K_0(\gamma_m b)} \cdot \frac{K_0(\gamma_m \rho)}{K_0(\gamma_n \rho)} \qquad [52]$$

for $W \leq \lambda_0/2$, $|J_0(\beta_m W/2)| \gtrless |J_0(\beta_n W/2)|$ according as $\beta_m \lesseqgtr \beta_n$ and

$$\frac{K_0(\gamma_n b)}{K_0(\gamma_m b)} \cdot \frac{K_0(\gamma_m \rho)}{K_0(\gamma_n \rho)} \gtrless 1 :$$

according as $\gamma_m \lesseqgtr \gamma_n$

Thus $A_m \gtrless A_n$ according as $\beta_m \lesseqgtr \beta_n$. In other words, the harmonic of the highest phase velocity has the highest amplitude.

The results of the last two sections 2.16 and 2.17 can be summarised as follows:

(i) The roots of the characteristic equation [30] are valid not only when the fundamental is considered but also when both the fundamental and space harmonics are taken into account provided $\beta_0 << \pi/l$. Then $2\pi m/l \pm \beta_0$ $(m > 0)$ give the roots of the characteristic equation [43].

(ii) The roots β_0 of equation [30] nearly equal to π/l, are not valid when the fundamental and space harmonic are considered as, in this case, the presence of the first order backward space harmonic should also be taken into account.

(iii) The harmonic of highest amplitude has the highest phase velocity and hence the lowest β_m. Thus, of all the terms of the characteristic equation, only one or two are of importance and these correspond to the values of m which are such that $k_0 < |\beta_m| < \pi/l$ or, $|\beta_m| \approx \pi/l$.

2.18. *Range of β_0 in class I when the Htgher Order Harmonics are present:*

The phase constant β_0 can vary between k_0 to ∞ (see section 2.11). When $\beta_0 = k_0$, b satisfies the equation $F_0(k_0 b) = 0$. When $\beta_0 = \infty$, b satisfies the equation $F_1(k_0 b) = 0$. When $F_0(k_0 b) = 0$ other roots of the characteristic equation [31] are given by equations [39] and [40]. When, in addition to the fundamental, space harmonics are considered, though the allowed range of values of β_0 is from k_0 to ∞, there exist different sub-ranges of β_0 in which different space harmonics have highest amplitudes. The orders m of the harmonics and the corresponding ranges of β_0 in which they have the highest amplitude are given in Table 2.

TABLE 2

The order m of the harmonic of relatively high amplitude and the corresponding range of β_0 $(\beta_0 \neq \beta'_m)$ (See Section 2.16.1)

Range of β_0	m
$k_0 < \beta_0 << \pi/l$	0
$\lvert\beta_0\rvert \approx \pi/l$	0, -1
$\pi/l << \beta_0 << 3\pi/l$	-1
$\lvert\beta_0\rvert \approx 3\pi/l$	-1, -2
$[(2n-1)\pi/l] << \beta_0 << [(2n+1)\pi/l]$	$-n$
$\lvert\beta_0\rvert \approx [(2n+1)\pi/l]$	$-n$, $-(n+1)$

In the case when $F_0(k_0 b) = 0$, the characteristic equation [30] has the roots $\beta_0 = (2\pi m/l) \pm k_0$, $m = 0, 1, 2, \ldots$ That is, the different values of β_0 corresponding to different values of m give the extreme values of β_m, viz., $|\beta_m| = k_0$

When $F_1(k_0 b) = 0$, the root $\beta_0 = \infty$ implies that either the harmonic of order infinity has the highest amplitude or the period l of the disc loading tends to zero in which case the fundamental has the highest amplitude The latter is a trivial case and the former is considered as a limiting condition at which the surface wave ceases to exist. The other roots of the characteristic equation when $F_1(k_0 b) = 0$ are given by equation [39] and [40].

Equation [39] has the roots

$$\beta_0 = (2\pi m/W) \approx (2\pi m/l), \quad m = 0, \pm 1, \pm 2, \ldots$$

Since these values of β_0 do not belong to any of the ranges defined in Table 1, they are of no interest. Equation [40] gives the root

$$\beta_0 = (4\,8/l), \quad (11.04/l), \quad (17.3/l), \text{ etc.}$$

Whether these roots are of any interest or not depends on the value of k_0. When β_0 belongs to the ranges defined in Table 1, the different roots of equation [40] correspond to different harmonics. However, the limiting value of β_m equal to π/l cannot be readily derived from the condition $F_1(k_0 b) = 0$.

2.19 *Power Flow for the Fundamental Harmonic*:

The total power flowing in the axial direction (z) is given by the relation

$$P_t = \tfrac{1}{2}\, Re \iint_A E_\rho \cdot H_\phi^*\, dA \qquad [53]$$

Where, A represents the cross-section transverse to the z-axis. The power flowing in the azimuthal direction is zero, since there is no magnetic field component in the axial direction. The power flowing in the radial direction is reactive, since in this case

$$\vec{E} \times \vec{H} = j \frac{k_0^2}{\omega \mu_0 \gamma_0} K_0(\gamma_0 \rho) K_1(\gamma_0 \rho) \cdot \vec{\rho} \qquad [54]$$

Where, $\vec{\rho}$ is the unit vector in the radial direction and the modified Bessel functions K_0 and K_1 are used as these have real values for real arguments.

$$P_t = \tfrac{1}{2} \int_b^s \int_0^{\pi 2} C_0^2 \frac{\beta_0}{\gamma_0} \cdot \frac{k_0^2}{\omega \mu_0 \gamma_0} (2/\pi)^2 K_1^2(\gamma_0 \rho)\, \rho\, d\rho\, d\phi \qquad [55]$$

The infinite integral converges since $\rho K_1^2(\gamma_0\rho)$ tends to zero as ρ tends to infinity. On integrating and simplifying, equation [55] reduces to

$$P_t = (\pi/2)(C^1/\gamma_0^2)[(\gamma_0 b)^2 K_0^2(\gamma_0 b) + 2\gamma_0 b K_1(\gamma_0 b) K_0(\gamma_0 b) - (\gamma_0 b)^2 K_1^2(\gamma_0 b)] \quad [56]$$

where

$$C^1 = C_0^2 - \frac{\beta_0 k_0^2}{\omega \mu_0 \gamma_0^2}\left(\frac{2}{\pi}\right)^2 \quad [57]$$

Consequently, the power flowing outside a radius ρ is obtained by putting $b = \rho$ in equation [56]. Hence, the percentage of power P^1 flowing outside the radius ρ is given by

$$P^1 = 100\,\frac{G(\gamma_0\rho)}{G(\lambda_0 b)} \quad [58]$$

where,

$$G(\gamma_0\rho) = (\gamma_0\rho)^2 K_0(\gamma_0\rho) + 2(\gamma_0\rho) K_0(\gamma_0\rho) K_1(\gamma_0\rho) - (\gamma_0\rho)^2 K_1^2(\gamma_0\rho) \quad [59]$$

Or, the percentage of power P_ρ contained within a radius ρ is given by

$$P_\rho = 100\left[1 - \frac{G(\gamma_0\rho)}{G(\gamma_0 l)}\right] \quad [60]$$

which indicates that P_ρ increases as γ_0 increases for any fixed value of $\rho - b$. That is, the power concentrates within a smaller region round the structure as the guide wavelength decreases.

In the two extreme cases when $\gamma_0 = 0$ and $\gamma_0 = \infty$, P_ρ is independent of ρ and becomes equal to ∞ and 0 respectively, since the fields themselves have the amplitudes ∞ and 0. As mentioned previously $\gamma_0 = 0$ is the condition for existence of a radiated wave and when $\gamma_0 = \infty$, the surface wave ceases to exist.

2.20 *Attenuation Constant for the Fundamental Harmonic*:

The attenuation constant α can be derived from the field components for the lossless case, using the usual perturbation technique and is given by

$$\alpha = \frac{P_d}{2P_t} \quad [61]$$

Where, P_t and P_d represent total power transmitted and power dissipated per unit legth of the structure and to simplify the evaluation, power dissipated from different parts of the structure is calculated independently.

Thus,

$$P_g = (P_1 + P_2 + P_3)/I \qquad [62]$$

Where,

P_1 = Power lost per period along the rim of the disc *i.e.*, in the region $\rho = b$.

P_2 = Power lost per period in the inner rod, *i.e.* in the region $\rho = a$, and

P_3 = Power lost per period along the surface of the discs, *i.e.*, in the region $a \leq \rho \leq b$

The expression for any P_r, $r = 1, 2, 3$ is given by

$$P_r = (\eta/2) \int_S \int H_\phi H_\phi^* \, dS \qquad [63]$$

where, H_ϕ^* is the complex conjugate of the tangential component of magnetic field H_ϕ and S is the surface over which H_ϕ is defined. η is the intrinsic impedance given by

$$\eta = \sqrt{\left(\frac{\omega \mu_0}{2 \sigma}\right)} \qquad [64]$$

where, σ is the conductivity of the structure material. Accordingly,

$$P_1 = \tfrac{1}{2} \eta \left[\int_0^{2\pi} \{H_\phi H_\phi^*\}_{\rho = b} \, b \, d\phi\right] (1 - W) \qquad [65]$$

Introducing the value of H_ϕ

$$H_\phi = C_0 \frac{k_0^2}{\omega \mu_0 \gamma_0} H_1^{(1)}(j \gamma_0 \rho) \exp(-j \beta_0 z)$$

equation [65] reduces to

$$P_1 = C_0^2 \, b \, \pi \, \eta \left[\frac{k_0^2}{\omega \mu_0 \gamma_0}\right]^2 [H_1^{(1)}(j \gamma_0 b)]^2 (1 - W) \qquad [66]$$

where

$$C_0 = \frac{\pi W B}{2I} \frac{J_0(\beta_0 W/2)}{H_0^{(1)}(j \gamma_0 b)}$$

Substituting equation [16], in equation [66], it reduces to

$$P_1 = \frac{B^2 \pi^3 W^2 \eta (1 - W) k_0^2 b}{4 I^2 \gamma_0^2} \frac{\epsilon_0}{\mu_0} \frac{K_1^2(\gamma_0 b)}{K_0^2(\gamma_0 b)} J_0^2(\beta_0 W/2) \qquad [67]$$

$$P_2 = \left[\frac{\eta}{2} \left\{ \int_0^{2\pi} H_\phi \, H_\phi^* \right\}_{\rho = a} a \, d\phi \right] W \qquad [68]$$

where,

$$H_\phi = j A \sqrt{\left(\frac{\epsilon_0}{\mu_0} \right)} F_1 (k_0 \rho) \exp (-j \beta_0 nl)$$

Thus (9)

$$P_2 = A^2 W \frac{\epsilon_0}{\mu_0} \eta F_1^2 (k_0 a) \pi a \qquad [69]$$

where

$$F_1 (k_0 a) = J_0 (k_0 a) \; Y_1 (k_0 a) - Y_0 (k_0 a) \; J_1 (k_0 a) = - \frac{2}{\pi k_0 a} \qquad [70]$$

$$A = \frac{B \pi}{2} F_0 (k_0 b)]^{-1} \qquad (21)$$

$$F_0 (k_0 b) = J_0 (k_0 a) \; Y_0 (k_0 b) - Y_0 (k_0 a] \; J_0 (k_0 b) \qquad (20)$$

Equation [69] reduces to

$$P_2 = \frac{B^2 \pi \, W \, \eta}{k_0^2 a} \frac{\epsilon_0}{\mu_0} \frac{1}{F_0^2 (k_0 b)} \qquad [71]$$

$$P_3 = \frac{\eta}{2} \int_a^b \int_0^{2\pi} H_\phi \, H_\phi^* \, \rho \, d\rho \, d\phi \qquad [72]$$

where, H_ϕ is given by equation [9] Thus,

$$P_3 = (B^2/8) [\pi^3 \eta / 8 F_0^2 (k_0 b)] (\epsilon_0 / \mu_0) [b^2 \{ F_1^2 (k_0 b) - F_0 (k_0 b) F_2 (k_0 b) \} - 4/(\pi^2 k_0^2)] \qquad [73]$$

where,

$$F_2 (k_0 b) = J_0 (k_0 a) \; Y_2 (k_0 b) - Y_0 (k_0 a) J_2 (k_0 b) \qquad [74]$$

and $F_0 (k_0 b)$, $F_1 (k_0 b)$ and A are given by equations [20], [25] and [21] respectively.

The total power transmitted (P_t) is given by (See equation 56)

$$P_t = (\pi \, C^1 / 2 \, \gamma_0^2) \; G (\gamma_0 b) \qquad [75]$$

where, C^1 is given by equation [57] and

$$G (\gamma_0 b) = (\gamma_0 b)^2 K_0^2 (\gamma_0 b) + 2 \gamma_0 \, b \, K_0 (\gamma_0 b) K_1 (\gamma_0 b) - (\gamma_0 b)^2 K_1^2 (\gamma_0 b) \qquad [76]$$

Substituting for C^1, equation [75] becomes,

$$P_t = \tfrac{1}{2} B^2 \pi W^2 \beta_0 k_0 \sqrt{(\epsilon_0/\mu_0)} \cdot G(\gamma_0 b)/(l^2 \gamma_0^4) \cdot [J_0 \beta_0 W/2)/[H_1^{(1)}(j\gamma_0 b)]^2 \quad [77]$$

The attenuation constant α determined from

$$\alpha = (P_1 + P_2) + P_3/2l P_t \quad [78]$$

is a function of the disc-radius b, the disc-spacing W and the phase constant β_0 of the fundamental harmonic. The nature of the dependence of α on b, W and β_0 is not apparent from equation [78] as it is complicated. The numerical computation in section 3 will however reveal the functional dependence of α on various physical parameters of the structure. The frequency dependence of α is discussed in section 3.

3. NUMERICAL RESULTS

The numerical evaluation of the roots of the characteristic equation, phase velocity, guide wavelength, etc., and their variation with parameters of the structure (b, w) is dealt with.

3.1 *Roots of the Characteristic Equation*:

The surface wave roots of the characteristic equation (for the fundamental harmonic)

$$\frac{2k_0}{l} \cdot \frac{J_0(\beta_0 W/2)}{\beta_0} \frac{\sin(\beta_0 W/2)}{} = -\gamma_0 \frac{K_0(\gamma_0 b)}{K_1(\gamma_0 b)} \cdot \frac{F_1(k_0 b)}{F_0(k_0 b)} \quad [31]$$

are determined by the successive bisection method with the aid of a digital computer (Elliott 803) for the following values of a, b $(l-w)$, λ_0 and k_0

a	:	Radius of the inner rod	= .25 cm
b	:	Radius of the disc	= .4 cm to 4 cms at intervals of 0.2 cm
W	:	Disc-spacing*	= 0.2 cm to 1.6 cm at intervals of 0.2 cm.
l-W	:	Thickness of the disc	= 0.047 cm
λ_0	:	Free-space wavelength	= 3.2 cm
k_0	:	Free-space wave number	= 1.9635 rad/cm

*The maximum value of W considered is only 1.6 cm ($= \lambda_0/2$) for reasons mentioned in the previous section.

The roots of the characteristic equation [31] are also determined for $b = 0.5$ cm. Discs of thie radius have been used for experimental verification. These roots are considered in a paper which is under publication [50] which deals with the comparative study of experimental and theoretical results.

The values of b for which a surface wave root exists and does not exist are given in Table 3. The values of b in the first and second coloumns of Table 3 are classified as class I aud class II respectively. The numerals inside the paranthesis (1), (2), (3) in this table refer to the different ranges of b belonging to class I.

The approximate ranges of b belonging to classes I and II can be determined from a plot of $g(\beta_0)$ versus b. $g(\beta_0)$ is given by the eqnation

$$g(\beta_0) = -\gamma_0 [K_0(\gamma_0 b)/K_1(\gamma_0 b)] \cdot [F_1(k_0 b)/F_0(k_0 b)] \quad [33]$$

It is seen from the plot of $g(\beta_0)$ versus b (Fig. 5) that for values of b approximately equal to 1.7 and 3.4 cms, $F_0(k_0 b) = 0$ and for the values of b approximately equal to 0.85, 2.5 and 4.15 cms, $F_1(k_0 b) = 0$ These values of b respectively correspond to the minimum and maximum values of β_0 in any range, (See section 2). In the former case, $\beta_0 = k_0$ and in the latter case $\beta_0 = \infty$. It has been pointed out that the values of b for which $\beta_0 = k_0$ represent a transition stage between classes I and II. Also, $\beta_0 = k_0$ is the condition for existence of a radiated wave. When $\beta_0 = \infty$, the surface wave cases to exist.

TABLE 3

Values of b for which a surface wave root exists (b belongs to class I) and does not exist (b belongs to class II) for the values of W considered *i.e.* $W = 0.2$ cm to 1.6 cms at intervals of 0.2 cm.

Values of b (cm) belonging to Class I	Values of b (cm) belonging to Class II
0.4 0.6 0.8 (1)	1 1.2 1.4 1.6 (1)
Hence, the range $0.4 \leq b \leq 0.8$	Hence, the range $1 \leq b \leq 1.6$
1.8 2 2.2 2.4 (2)	2.6 2.8 : 3.2 (2)
Hence, the range $1.8 \leq b \leq 2.4$	Hence, the range $2.6 \leq b \leq 3.2$
3.4 3.6 3.8 4 (3)	
Hence, the range $3.4 \leq b \leq 4$	

The effect of b on the propagation characteristics obtained from a study Fig. 5 is summerised in Table 4.

The variation of the root β_0 as a function of b and W is shown in Figs. 6 and 7, respectively. In these figures the numerals in the parenthesis (1), (2), and (3) correspond to different ranges of b belonging to class I. The following observation can be made from Figures 6 and 7.

In any range b,

(i) β_0 increases with b for any fixed value of W

(ii) plots of β_0 versus b become steeper as W is decreased and are similar in different ranges of b.

(iii) plots of β_0 versus W are also similar in different ranges of b and give straight lines for the smallest value of b in the ranges (2) and (3).

(iv) β_0 decrease with W in general. When it increases with W, the increase is very small.

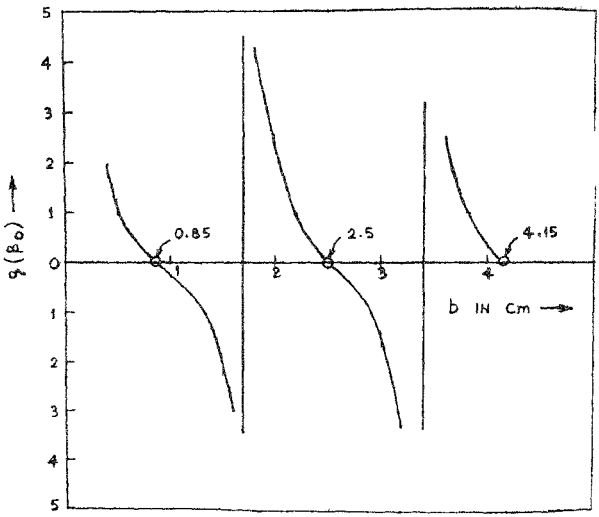

FIG. 5

Plot of $g(\beta_0)$ verses b [see eq. (2.38)]
b: Disc-radius
β_0: Phase constant for the fundamental harmonic =2.3636 radians/cm.

TABLE 4

Effect of b on the propagation characteristics

b in cms.	Effect on the propagation characteristic
$a<b<0.85$ $1.7<b<2.5$ $3.4<b<4.15$	The structure supports a surface wave with $v_p<0$. The ranges of b belong to Class I.
$b=0.85$ $b=2.5$ $b=4.15$	Correspond to a limiting case when the surface wave ceases to exist ($v_p=0$).
$0.85<b<1$ $2.5<b<2.6$	A part of the interval [corresponding to $F_1(k_0b)/F_0(k_0b)$ being very small] belongs to class I. The remaining part belongs to class II.
$1<b<1.7$ $2.6<b<3.4$	The strucsure does not support a surface wave. The ranges of b belong to class II.
$b=1.7$ $b=3.4$	Represent the transition stage between classes I and II. $v_p=c$.

3.2 *Delay Radio and Guide Wave length for the Fundamental Space Harmonic.*

The propagation characteristics of the structure can be further studied in terms of guide wavelength λ_g and the delay ratio c/v_p, where v_p is the phase velocity.

The following conclusion can be draw from Figures 6 and 7.

(i) Considering the three different ranges of b belonging to class I (See Table 3) *viz.*, (1) $b=0.4$ cm to 0.8 cm, (2) $b=1.8$ cm to 2.4 cm and (3) $b=3.4$ cm to 4 cm, in each range,

(*a*) λ_g decreases and c/v_p increases with increasing b, for any fixed value of W.

(*b*) λ_g increases and c/v_p decreases with inceseasing W, for any fixed value of b except in the following case (ii).

(ii) λ_g decreases and c/v_p increases when W is increased from 0.2 to 0.4 cms for $b=0.4$, 1.8, 2. 3.4., 3.6 and 3.8 cms.

(iii) In any range of b, the minimum value of λ_g and maximum value of c/v_p occur for the largest value of b and the smallest value of W.

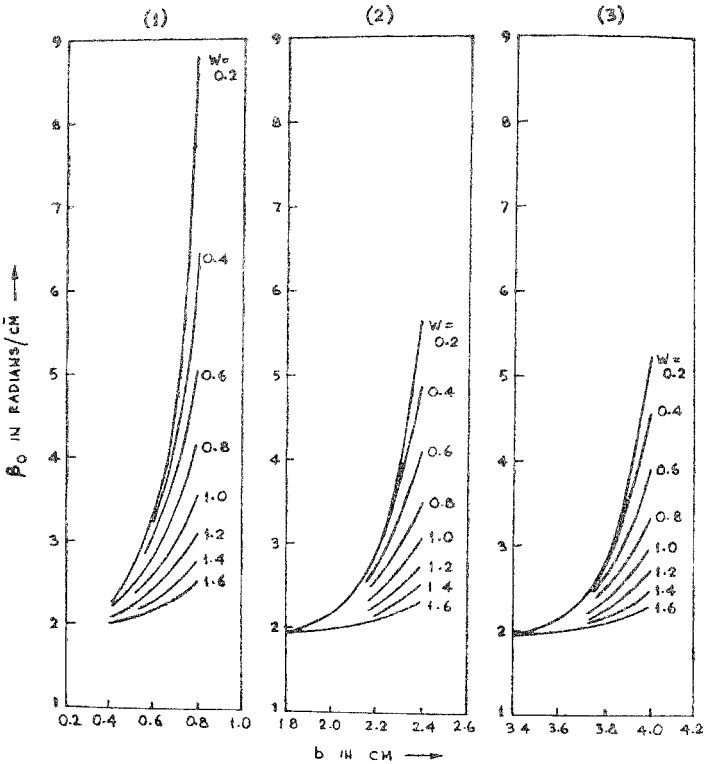

FIG. 6

Plots of β_0 versus b for different values of W.
β_0: Axial phase constant
b: Disc-radius
W: Disc-spacing in cm.
λ_0: Free space wavelength = 3.2 cm.
See table 4.1 for the definition of ranges (1), (2) and (3).

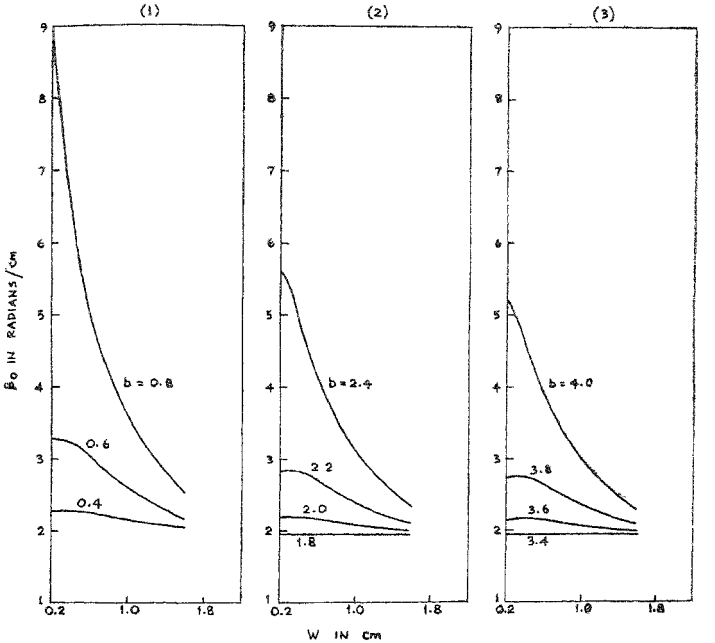

FIG. 7

Plots of β_0 versus W for different values of b.
β_0: Axial phase constant; W: Disc-spacing
b: Disc-radius in cm.; λ_0: Free space wavelength = 3.2 cm.
See table 4.1 for the Definition of ranges (1), (2) and (3).

(iv) The minimum values of λ_g and the corresponding maximum values c/v_p in different ranges are

λ_g min.	= 0.7219327	In the range (1)
c/v_p max.	= 4.49316	
λ_g min.	= 1.1093822	in the range (2)
c/v_p max.	= 2.884488	
λ_g min.	= 1 2026836	in the range (3)
c/v_p max.	= 2,660716	

Thus the minimum value of λ_g increases from range to range and the maximum value of c/v_p decreases from range to range

(v) Of all the values of b and W considered, the lowest guide wavelength and hence the highest delay ratio correspond to $b=0.8$ cm and $W=0.2$ cm.

(vi) In any range, the maximum value of λ_g and the minimum value of c/v_p occur for the smallest value of b and the largest value of W.

(vii) The maximum value of λ_g and the minimum value of c/v_p in different ranges are

$\left.\begin{matrix}\lambda_g \text{ max.} & =3.0913437\\ c/v_p \text{ min.} & =1.035148\end{matrix}\right\}$ in the range (1)

$\left.\begin{matrix}\lambda_g \text{ max.} & =3.1985603\\ c/v_p \text{ min.} & =1.001722\end{matrix}\right\}$ in the range (2)

$\left.\begin{matrix}\lambda_g \text{ max.} & =3.1983437\\ c/v_p \text{ min} & =1.002039\end{matrix}\right\}$ in the range (3)

(viii) The largest guide wave length and hence the smallest delay ratio therefore correspond to $b=1.8$ cm and $W=1.6$ cm.

It may be noted that in any range of b, the value of b for which λ_g is minimum and c/v_p is maximum, lies in the vicinity of a root of $F_1(k_0 b)=0$ (See Fig. 5 and Table 4) and the value of b for which λ_g is maximum and c/v_p is minimum lies in the vicinity of a root $F_0(k_0 b)=0$. The roots of $F_1(k_0 b)=0$ give the root $\beta_0=\infty$ or $\lambda_g=0$ and $c/v_p=\infty$ (See section 2.11). The roots of $F_0(k_0 b)=0$ or $\lambda_g=\lambda_0$ and $c/v_p=1$. The exact values of b for which the characteristic equation [31] has the roots $\beta_0=\infty$ and $\beta_0=k_0$ are not included in Table 3. However, the values of b giving maximum and minimum values of λ_g lie in the vicinity of the roots of $F_0(k_0 b)=0$ and $F_1(k_0 b)=0$ respectively. The maximum value of λ_g is nearly equal to λ_0

3.3 *Field Component E_ρ of the Fundamental Harmonic.*

The radial field component E_ρ of the fundamental harmonic is given by

$$E_\rho = C_0 \frac{\beta_0}{\gamma_0} H_1^{(1)}(j\gamma_0\rho)\exp(-j\beta_0 z) \qquad [42]$$

Plots of the field component E_ρ normalised with respect to the field amplitude at a distance of 1 mm from the structure are shown in Figures 8-10.

The normalised field amplitude is given by the relation

$$\left|E_\rho\right|_{\text{norm}} = \frac{K_1(\gamma_0\rho)}{K_1[\gamma_0(b+\cdot 1)]}, \quad \rho \geq b+0.1 \qquad [79]$$

The following remarks may be made from Figures 8-10. (These also follow from the plots of β_0 versus b and W).

(*a*) In any range of b,

(i) the rate of decay of the field components in the radial direction increases as b increases for any fixed value of W.

(ii) the rate of decay decreases as W increases for any fixed value of b.

(iii) maximum rate of decay and the minimum field spread correspond to the largest value of b and the smallest value of W.

(iv) minimum rate of decay and maximum field spread correspond to the smallest value of b and the largest value of W.

Of all the structure parameters considered, minimum field spread correspond to $b=0.8$ cm and $W=0.2$ cm. and maximum field spread correspond to $b=1.8$ cm. and $W=1.6$ cm.

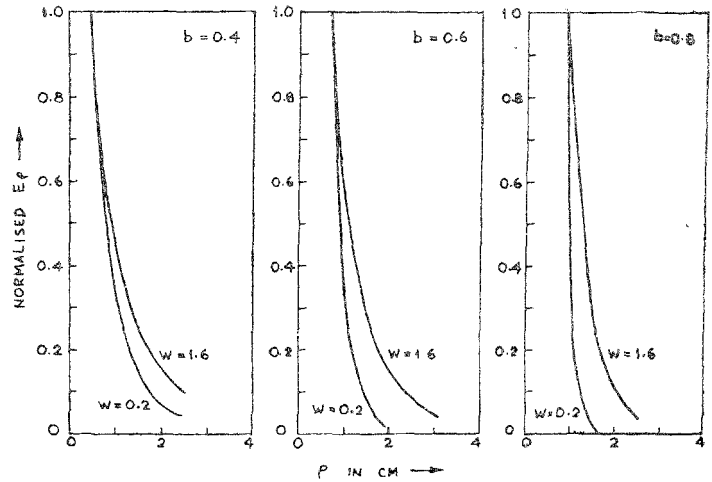

FIG. 8

Field plots for the component E_ρ.
b: Disc-radius in cm.
W: Disc-spacing in cm.
ρ. Distance measured from the axis of the structure.

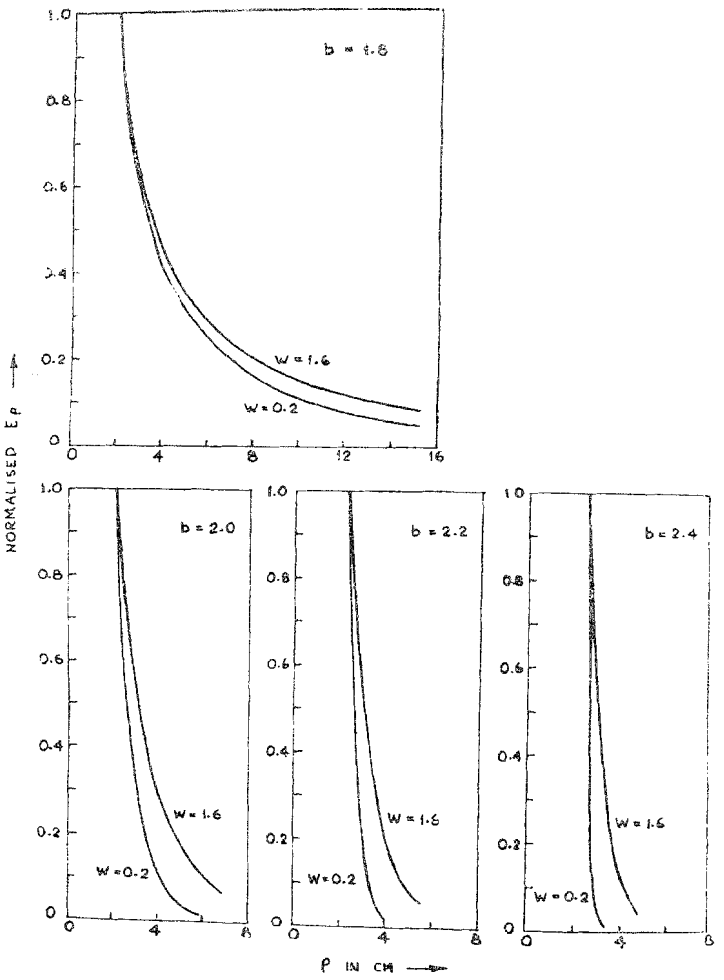

FIG. 9

Field plots for the component E_ρ

b: Disc-radius in cm W: Disc-spacing in cm. ρ. Distance measured from the axis of the structure.

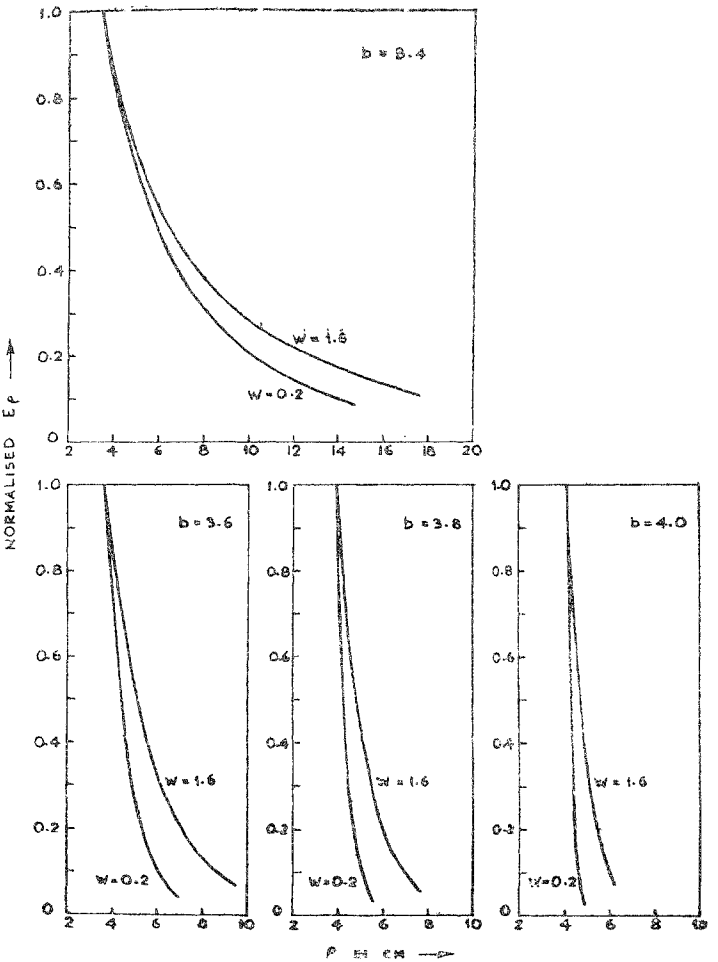

FIG. 10

Field plots for the component E_ρ.
b: Disc-radius in cm. W: Disc-spacing in cm. ρ: Distance measured from the axis of the structure.

3·4 *Dispersion characteristics for the Fundamental Harmonic*

The effect of variation of the frequency of excitation on the propagation characteristics of the structure is determined by solving the characteristic equation (31) for the following range of values of k_0

$k_0 - 0{\cdot}8$ radians/cm. to $4{\cdot}8$ radians/cm. in steps of $0{\cdot}4$ radians/cm.

This corresponds to a frequency range of 3·82 *GHZ* to 22·93 *GHZ* in steps of 1·91 $G H_z$. The values of b considered are those belonging to the ranges (1) and (2) (See Table 3) only one value of W. *viz*., $W = 0{\cdot}2$ cm. is considered for simplicity.

Table 5 gives the values of b and k_0 for which the structure can support a surface wave. The values of k_0 for which the structure supports a surface wave belong to the pass-band. The values of k_0 for which the structure does not support a surface wave belong to the stop-band.

Figures 11 and 12, 13 and 14 represent the plots of β_0 versus k_0 and λ_g/λ_0 versus k_0 respectively. (It is to be noted that plots are not made in the pass-bands which contain only one value of k_0 (See Table 5). The following conclusions can be drawn from these plots

(i) The whole range of k_0 considered belongs to pass-band for $b = 0.4$ cm.

(ii) The number of pass-bands increases with increasing b.

(iii) In any band the ratio λ_g/λ_0 decreases with increasing k_0.

(iv) The rate of decay of λ_g/λ_0 with respect to k_0 decreases with increasing b in the range (1) (See Table 3).

(v) The rate of decay of λ_g does not vary significantly as b is varied in range (2) (See Table 3).

(vi) For any fixed value of b, the rates of decay in different bands are nearly equal.

3·5 *Effect of Higher Order Space Harmonics.*

The effect of higher order hormonics on the roots of the characteristic equation is studied by solving the following equation

$$\frac{2 k_0}{l}\left[\frac{J_0(\beta_0 W/2)}{\beta_0 \gamma_0}\frac{\sin(\beta_0 W/2)}{}\frac{K_1(\gamma_0 b)}{K_0(\gamma_0 b)} + \frac{J_0(\beta_{-1} W/2)}{\beta_{-1}}\frac{\sin(\beta_0 W/2)}{\gamma_{-1}}\frac{K_1(\gamma_{-1} b)}{K_0(\gamma_{-1} b)}\right] = -\frac{F_1(k_0 b)}{F_0(k_0 b)} \qquad [80]$$

which is obtained from equation (30) β_{-1} and γ_{-1} are respectively the axial and radial propagation constants of the first order backward space harmonic. It is necessary to consider only the roots β_0 such that $k_0 < \beta_0 < \pi/l$ (See section 2·16). This requires the maximum value of W to be restricted to 1·4 cm. (Table 3.)

TABLE 5

Values of k_0, the corresponding frequency and b for which surface wave roots exist ($W = 0.2$ cm.)

b cms	Range of k_0 in rad/cm. and frequency (f) in $G\,Hz$
0·4	$k_0 =$ 0·8 to 4·8 in steps of 0·4 $f =$ 3·82 to 22·93 in steps of 1·91
0·6	$k_0 =$ 0·8 to 3·6 in steps of 0·4 $f =$ 3·82 to 17·19 in steps of 1·91
0·8	$k_0 =$ 0·8 to 2 in steps of 0·4 $f =$ 3·82 to 9·55 in steps of 1·91
1·8	$k_0 =$ 2 to 2·8 in steps of 0·4 $f =$ 9·55 to 13·38 in steps of 1·91 $k_0 =$ 4·4, 4·8 $f =$ 21·01, 22·94
2	$k_0 =$ 1·6 to 2 in steps of 0·4 $f =$ 7·64 to 9·55 in steps of 1·91 $k_0 =$ 3·6 to 4·8 in steps of 0·4 $f =$ 17·19 to 22·94 in steps of 1·91
2·2	$k_0 =$ 2, 2·4 $f =$ 9·55, 11·47 $k_0 =$ 3·2 to 4 in steps of 0·4 $f =$ 15·29 to 19·1 in steps of 1·91 $k_0 =$ 4·8 $f =$ 22·94
2·4	$k_0 =$ 1·6, 2 $f =$ 7·64, 9·55 $k_0 =$ 3·2 $f =$ 15·29 $k_0 =$ 4·4, 4·8 $f =$ 21·01, 22·94

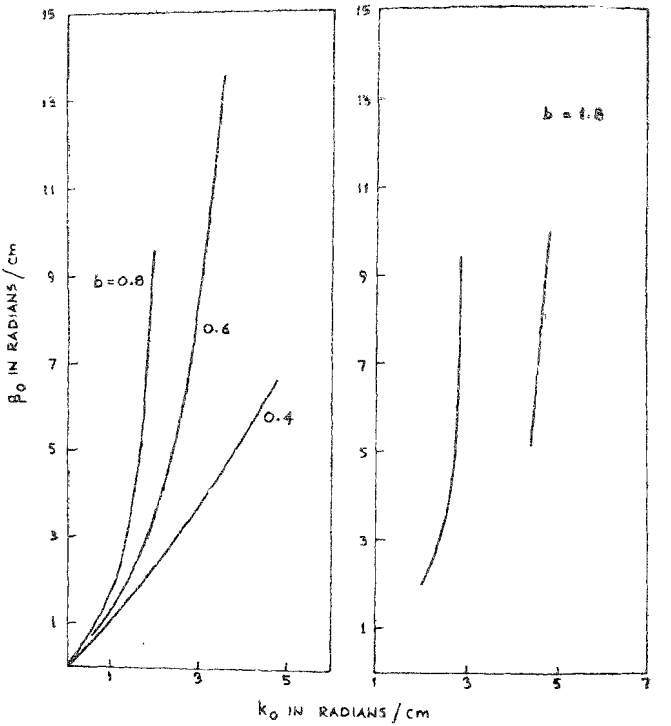

FIG. 11

Dispersion diagram for the fundamental harmonic.
β_0: axial phase constant; W: Disc-spacing=0.2 cm.
k_0: Free space wave number; b: Disc-radius in cm.

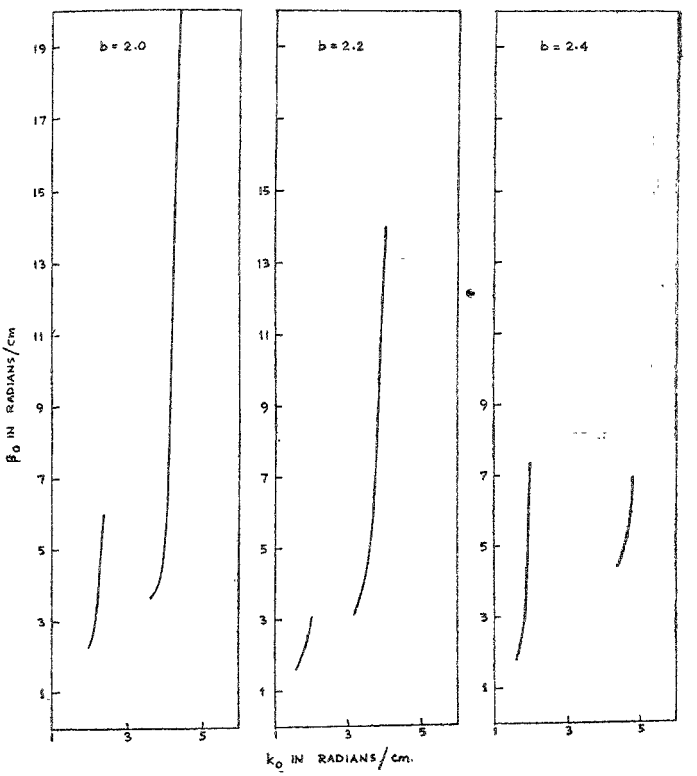

FIG. 12

Dispersion diagram for the fundamental harmonic.
β_0: axial phase constant; W: Disc-spacing=0.2 cm.
k_0: Free space wave number; b: Disc-radius in cm.

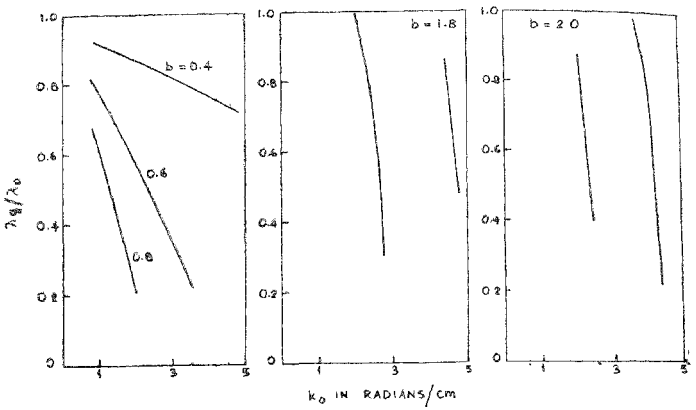

FIG. 13

Plots of λ_g/λ_0 versus k_0.
b : Disc-radius in cm ; λ_g : Guide wavelength in cm.
W : Disc-spacing=0.2 cm ; λ_0 : Free space wavelength in cm.
k_0 : Free space wave number.

Tables 1 to 3 of the Appendix contain the values of β_0 and β_{-1} obtained from equation (80). The roots of β_0 of the equation (31) for the fundamental harmonic are given in the same table for the sake of comparison.

The following observations* can be made regarding the roots β_0 and β_{-1} (contained in Tables 1 to 3)

(i) $\beta_{-1} >> \beta_0$ for almost all values of b when W is small

(ii) For any value of b, $\beta_{-1} \sim \beta_0$ decreases as W increases

(iii) For any value of b in any range, the largest value of W for which a root is given in the tables decreases as b is increased.

(iv) The difference $\beta_{-1} \sim \beta_0$ is minimum in range (1) for the smallest value of b and the largest value of W (b=0.8 cm. and W=1 cm.). In the ranges (2) and (3), $\beta_{-1} \sim \beta_0$ is minimum for the largest value of W and the second smallest value of b (W=1.4 cm, b=2 cm and b=3.6 cm).

* Statements (i) to (iv) refer to the roots of equation (80).

(v) The value of the root β_0 computed from equation (31) is always less than that computed from equation (80).

(vi) The difference between the two values of β_0 is, in general very small when W is small.

(vii) For any value of b, the difference between the two values of β_0 increases as W increases.

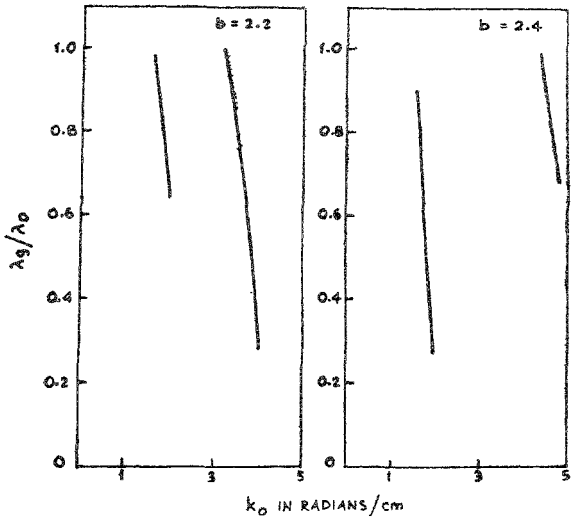

FIG. 14

Plots of λ_g/λ_0 versus k_0
λ_g: Guide wavelength in cm
λ^0: Free space length in cm
b: Disc-Radius in cm
W: Disc-spacing=0 2 cm
k_0: Free space wave number

3 6 *Relative Amplitudes of E_z for $m=0$ and $m=-1$.*

The ratio (R^1) of the amplitude A_0 of the fudamental harmonic to that of the first order backward space harmonic A_{-1} for the field component E_z is given by

$$R^1 = \frac{A_0}{A_{-1}} = \left| \frac{J_0(\beta_0 W/2)}{J_0(\beta_{-1} W/2)} \right| \cdot \frac{K_0(\gamma_{-1} b)}{K_0(\gamma_0 b)} \quad \frac{K_0(\gamma_0 \rho)}{K_0(\gamma_{-1} b)} \qquad [81]$$

which is obtained from equation (52).

The ratio A_0/A_{-1} has been computed from equation (51) for different values of b and W and the corresponding values of β_0 and β_{-1} (Tables 1 to 3)

Plots of A_0/A_{-1} versus ρ for different values of b and W are given in Figures 15 and 16 It can be seen that

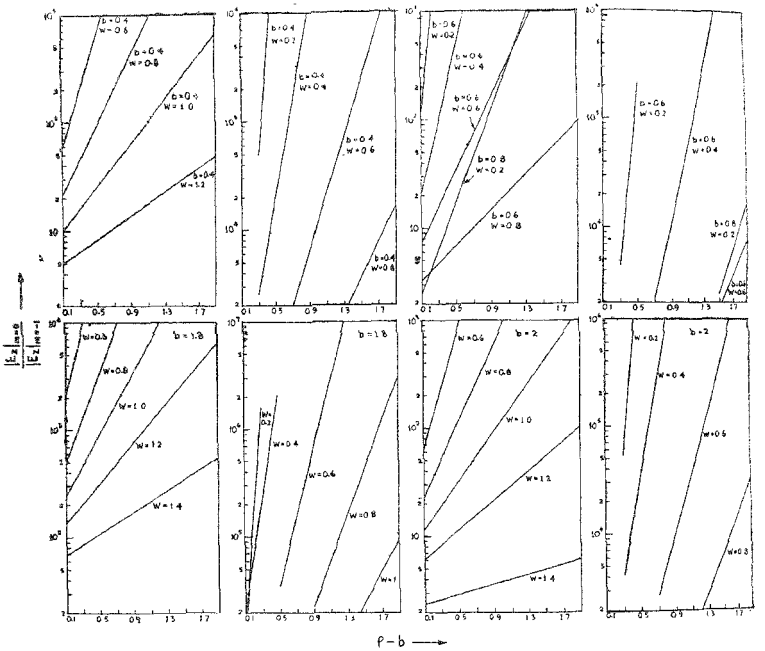

FIG. 15

Plots of relative amplitudes of E_z for $m=0$ and $m=-1$ versus distance (in cm) from the structure.
b=disc-radius in cm.
W=disc-spacing in cm.
ρ=distance from the axis.

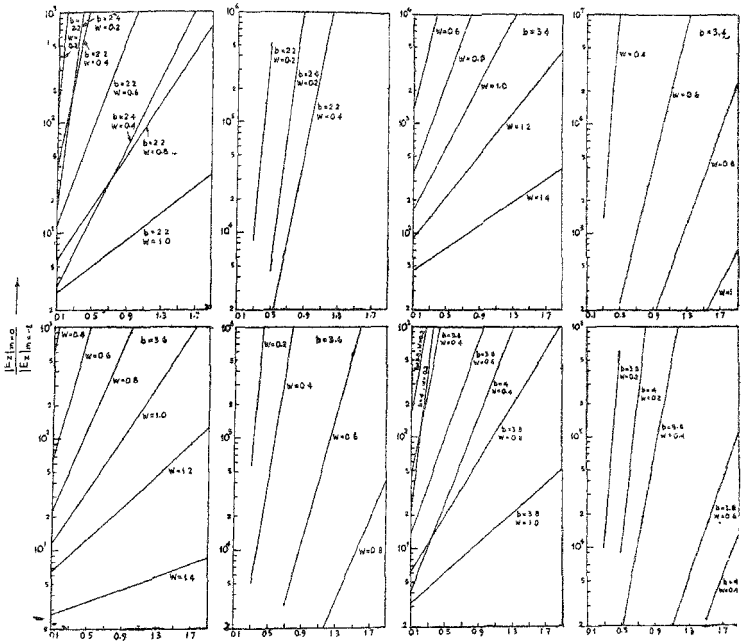

FIG. 16

Plots of relative amplitudes of E_z for $m=0$ and $m=-1$ versus distance (in cm.) from the structure.
b=disc-radius in cm.
W=disc-spacing in cm.
ρ=distance from the axis.

(i) R^1 increases with ρ which means that the fundamental harmonic is more predominant that the first order backward space harmonic at larger distances from the structure.

(ii) for small values of W, A_0/A_{-1} is very large.

(iii) for any values of b, A_0/A_{-1} decreases as W is increased.

The effect of b on the relative amplitudes of space harmonics is summarised in Table 6.

3.7 *Power Flow for the Fundamental Harmonic.*

The percentage of power flowing in the axial direction within a radius ρ is given by the relation

$$P_\rho = 100 \left[1 - \frac{G(\gamma_0 \rho)}{G(\gamma_0 b)} \right] \qquad [60]$$

where,

$$G(\gamma_0 \rho) = (\gamma_0 \rho)^2 K_0^2(\gamma_0 \rho) + 2\gamma_0 \rho K_0(\gamma_0 \rho) K_1(\gamma_0 \rho) - (\gamma_0 \rho)^2 K_1^2(\gamma_0 \rho)$$

Figures 17 to 19 show the plots of P_ρ versus W for different values of b and ρ. It is observed that, in general, P_ρ is a decreasing function of W.

TABLE 6

Effect of b and W on the relative amplitudes of harmonics

b in cm	W in cm	Relative magnitudes of A_m
0.4	$0.2 \leq W \leq 1.4$	$A_0 > A_m$
	$W = 1.6$	$A_{-1} > A_m$
0.6	$0.2 \leq W \leq 1.2$	$A_0 > A_m$
	$W = 1.4, 1.6$	$A_{-1} > A_m$
0.8	$W = 0.2, 0.4$	$A_0 > A_m$
	$0.6 \leq W \leq 1.6$	$A_{-1} > A_m$
1.8	$0.2 \leq W \leq 1.4$	$A_0 > A_m$
	$W = 1.6$	$A_{-1} > A_m$
2	$0.2 \leq W \leq 1.4$	$A_0 > A_m$
	$W = 1.6$	$A_{-1} > A_m$
2.2	$0.2 \leq W \leq 1.4$	$A_0 > A_m$
	$W = 1.6$	$A_{-1} > A_m$
2.4	$0.2 \leq W \leq 0.8$	$A_0 > A_m$
	$1 \leq W \leq 1.6$	$A_{-1} > A_m$
3.4	$0.2 \leq W \leq 1.4$	$A_0 > A_m$
	$W = 1.6$	$A_{-1} > A_m$
3.6	$0.2 \leq W \leq 1.4$	$A_0 > A_m$
	$W = 1.6$	$A_{-1} > A_m$
3.8	$0.2 \leq W \leq 1.4$	$A_0 > A_m$
	$W = 1.6$	$A_{-1} > A_m$
4	$0.2 \leq W \leq 1$	$A_0 > A_m$
	$0.2 \leq W \leq 1.6$	$A_{-1} > A_m$

Note: $\beta_0 < \pi/l$ when $A_0 > A_m$ and $\beta_0 > \pi/l$ when $A_{-1} > A_m$.

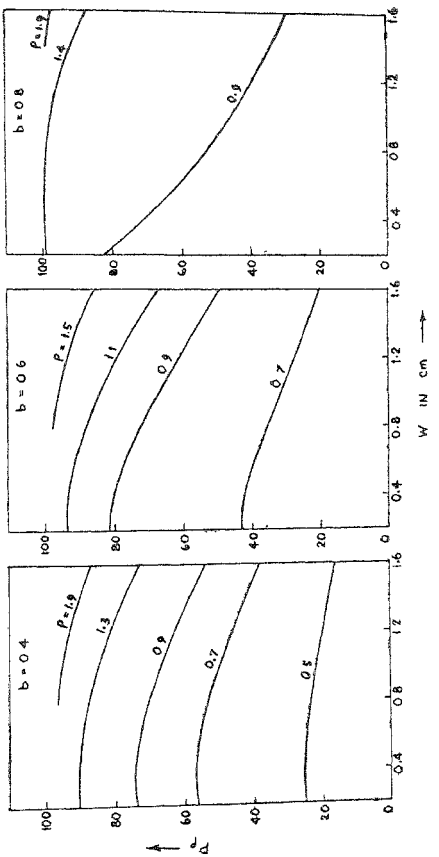

FIG. 17

Plots of P_ρ ve.sus W.

P_ρ : Percentage of power flowing within a radius ρ (cm)

b : Disc-radius in cm.

W : Disc-spacing.

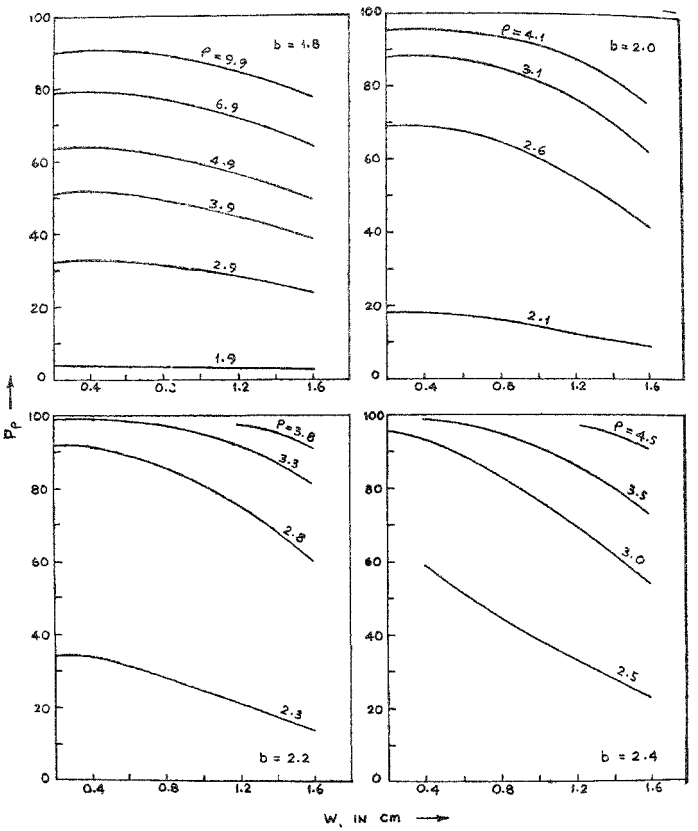

FIG. 18

Plots of P_ρ versus W.
P_ρ : Percentage of power flowing within a radius ρ (cm.)
b: Disc-radius in (cm.)
W: Disc-spacing

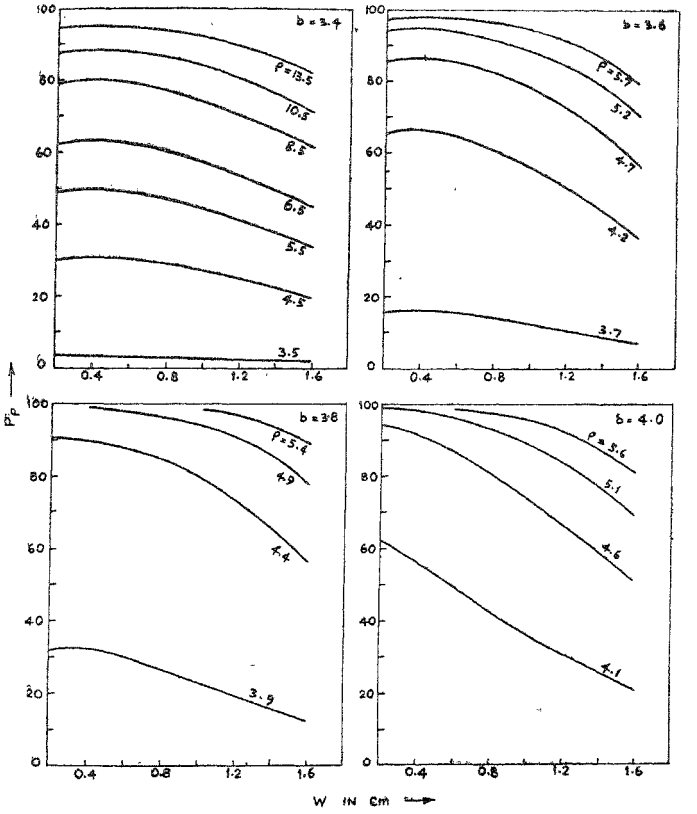

FIG. 19

Plots of P_ρ versus W.
P_ρ: Percentage of power flowing within a radius ρ (cm.)
b: Disc-radius in cm.
W: Disc-spacing

3.8 *Evaluation of the attenuation Constant* α

The attenuation constant α is determined from

$$\alpha = \frac{P_1 + P_2 + P_3}{2\,I\,P_t} \qquad [78]$$

Where, P_1, P_2, P_3 and P_t are given by equation [67], [71], [73] and [77] respectively.

The following values have been assumed for the constants σ, ϵ_0 and μ_0.

σ : Conductivity of copper : 5.8×10^5 mhos/cm

ϵ_0 : Permittivity of free space ; 8.854×10^{-14} Farad/cm

μ_0 ; Permittivity of free space : $4\pi \times 10^{-9}$ Henry/cm

Plots of α versus W for different values of b are shown in Figure 20 which leads to the following conclusions :

In any range :

(i) the attenuation constant α increases as b increases for any fixed value of W.

(ii) α decreases with increasing W for any fixed value of b.

(iii) minimum attenuation occurs in structures with minimum value of b and maximum value of W.

(iv) maximum attenuation occurs on a structure with maximum value of b and minimum value of W.

The maximum and minimum values of α are given in Table 7. It is seen that α_{max} decreases from ranges (1) to (2) and increases from ranges (2) to (3), whereas, α_{min} decreases continuously from ranges (1) to (3).

TABLE 7

α_{max} and α_{min}

Range of b	b in cm	W in cm	α_{max} in nepers/cm.	α_{min} in nepers/cm.
(1)	0.8	0.2	0.118658×10^{-1}	.....
	0.4	1.6	.....	0.430446×10^{-4}
(2)	2.4	0.2	0.935601×10^{-2}	.....
	1.8	1.6	.....	0.653606×10^{-5}
(3)	4	0.2	0.12207×10^{-1}	.....
	3.4	1.6	.....	0.64682×10^{-5}

3.9 *Variation of* α *with Frequency.*

The variation of α with frequency is studied by computing the values of α from equation (78) for different values of k_0 and the corresponding values of β_0. Plots of α versus k_0 are given in Figures 21 and 22. It is obvious that α increases with frequency.

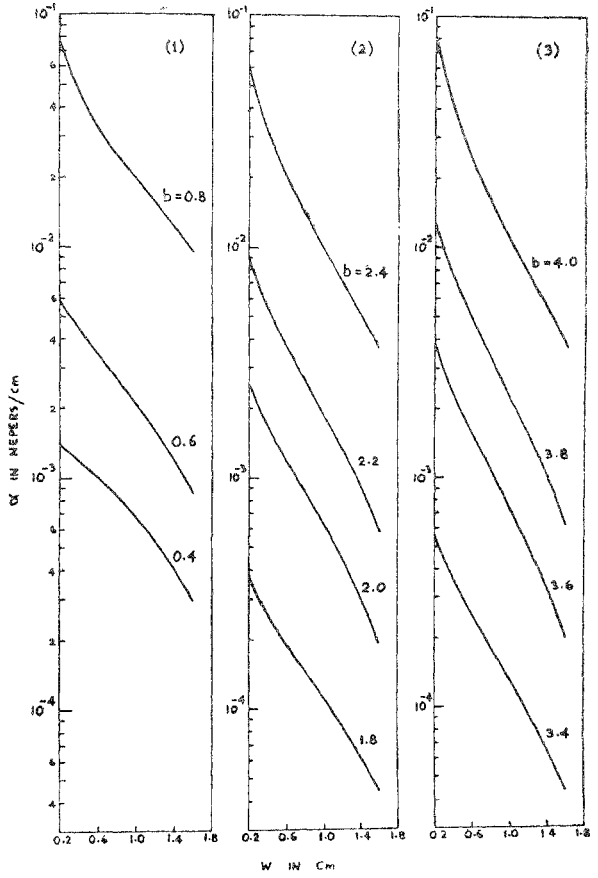

FIG. 20

Plots of attenuation constant α versus W.
W: Disc-spacing
b: Disc-radius in cm.
λ_0: Free spacing wave length = 3.2 cm.
See table 4.1 for ranges (1), (2) & (3).

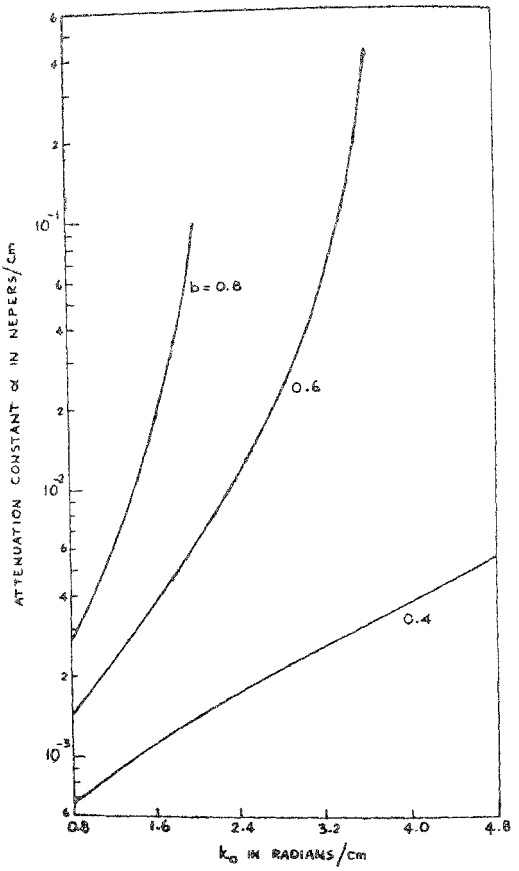

FIG. 21

Variation of α with k_0.
b: Disc-radius in cm.
W: Disc-spacing=0.2 cm.
k_0: Free space wave number.

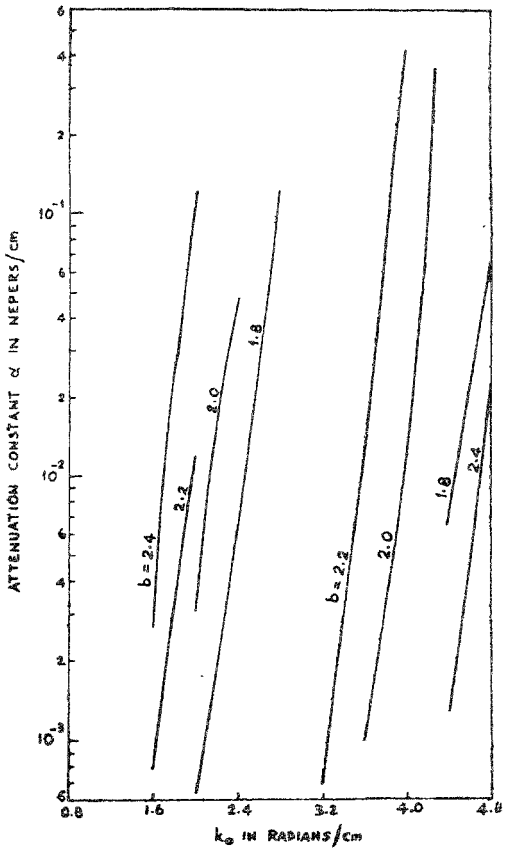

FIG. 22

Variation of α with k_0.
b: Disc-radius in cm.
W: Disc-spacing=0.2 cm.
k_0: Free space wave number

APPENDIX

TABLE 1

Root $\beta_0^{(2)}$ of the characteristic equation [30], 1st value.
(When the existence of the first order backward space harmonic is taken into account).

$\beta_{-1}^{(2)}$: phase constant of the first order backward space harmonic, 2nd value.

$\beta_0^{(1)}$: Root of the characteristic equation [31], 3rd value.

b: disc-radius W = dis-spacing

W in cms.	b in cms		
	0.4	0.6	0.8
0.2	2.2591	3.32086	10.29134
	23.17885	22.11714	15.14666
	2.2589522	3.3142470	8.8223036
	2.27298	3.27238	
0.4	11.78336	10.78396	
	2.2727705	3.2538756	6.5287367
0.6	2.24614	3.07966	
	7.46512	6.6316	
	2.1448904	3.0281279	5.0972945
0,8	2.2055	2.91154	
	5.21258	4.50662	
	2.2016848	2.7957136	4.1940993
	2.16310		
1.0	3.838032		
	2.1541235	2.5929655	3.5792708
	2.12774		
1.2	2.910981		
	2.1081694	2.4245809	3.1357619
1.4			
	2.0670798	2.2879881	2.8023634

APPENDIX—(*contd.*)

TABLE 2

Root $\beta_0^{(2)}$ of the characteristic equation [30] 1st value.
(when the existence of the first order backward space harmonic is taken into account).

$\beta_{-1}^{(2)}$: Phase constant of the first order backward space harmonic, 2nd value.

$\beta_0^{(1)}$: Root of the characteristic equation [31], 3rd value.

b : disc-radius W = disc-spacing

W in cms.	b in cms.			
	1.8	2.0	2.2	2.4
	1.96666	2.16774	2 84186	5.80336
0.2	23.47134	23 27026	22.59614	19.63434
	1.9666588	2.1675894	2 8388579	5.6636794
	1.96686	2.18112	2 84252	5.27434
0.4	12 08948	11 87522	11 21382	8.782
	1 9668776	2.1810149	2.8353941	4 8748824
	1.96666	2.1609	2.71924	
0 6	7.74460	7.55036	6.99202	
	1.9666758	2.1599859	2.6971739	4.0860549
	1.96663	2.12944	2 58748	
0.8	5.45186	5.28872	4.83068	
	1 9662861	2.1264975	2 5385054	3.5066084
	1.96582	2.09634	2 49166	
1.0	4 03531	3.90479	3.50947	
	1 9658036	2 0899321	2.3931166	3.0823378
	1 9653	2 06778		
1 2	3 07334	2.97086		
	1.9652937	2.0554430	2.2700041	2.7641264
	1 96482	2.05848		
1.4	2 37739	2.28373		
	1 9648068	2.0257939	2.1702208	2 5204420

APPENDIX—(*concld*)

TABLE 3

Root $\beta_0^{(2)}$ of the characteristic equation [30], 1st value.
(when the existence of the first order backward space harmonic is taken into account)

$\beta_{-1}^{(2)}$: Phase constant of the first order backward space harmonic, 2nd value.

$\beta_0^{(1)}$: Root of the characteristic equation [31], 3rd value

b : disc-radius W = disc-spacing

W in cms.	b in cms.			
	3 4	3.6	3.8	4.0
	1 9675	2 14442	2 75522	5.32162
0 2	23 4705	23.29358	22.68278	20.11638
	1.9674991	2.1443018	2.7527022	5.2243046
	1.96782	2.15742	2.7623	4 87294
0 4	12.08852	11.89892	11.29404	9.18340
	1.9678001	2.1573416	2.7565504	4 6040083
	1 96754	2.13898	2 6511	
0 6	7 74372	7.57228	7.06016	
	1.9675218	2.1381493	2.6326995	3.910713
	1.96695	2.10998	2 5283	
0.8	5 45118	5.30818	4 88986	
	1.9669900	2.1073290	2.4871411	3.3838332
	1.96634	2·07946	2.43322	
1.0	4 03479	3.92167	3.56791	
	1.9663419	2.0737589	2.3524649	2.9918257
	1.96570	2.05206		
1 2	3 07294	2.98558		
	1.9656711	2.0423495	2 2381041	2.6954176
	1.9651	2.04142		
1.4	2.37711	3.30079		
	1 9650466	2.0157274	2.1457167	2.4677260

6. Acknowledgment

The authors are grateful to Dr. S. Dhawan for giving all facilities to conduct the work. They are also thankful to the Professor-in-charge for encouragement and to Mr. S. K. Sen for computational work The authors express their deep gratitude to Dr. James, R. Wait, Senior Scientist O/T ITS for his technical advice towards this project. The authors are thankful also to U.S. Department of Commerce and U.G.C., New Delhi, for the PL-480 contract and necessary facilities.

References

1. Sommerfeld, A. . . . . *Ann. der. Phys.*, 1909, **28**, 665
2. ——— . . . . *Wied Ann. Phys , U. Chemie*, 1899, **67**, 233.
3. Zenneck, J. . . . . *Ann der. Phys.*, 1899, **23**, 846.
4. Harms, F. . . . . *Ibid.*, 1907, **23**, 44
5. Hondros, D. . . . . *Ibid.* 1909, **30**, 905.
6. ——— and Debye, P. . . *Ibid*, 1910, **32**, 465.
7. Weyl, H. . . . . *Ibid*, 1919, **60**, 481.
8. Roif, B. . . . . *Pro. I.R.E.*, 1930, **18**, 391.
9. Kahan, T. and Eckart, G. . . *Physical Review*, 1949, **76**, 406
10. Bouwkamp, C. J. . . . . *Ibid*, 1950, **80**, 294.
11. Burrows, C. R. . . . . *Proc. I.R.E.*, 1937, **25**, 219.
12. Goubau, G. . . . . *J Appl. Phy.*, 1950, **21**, 1119.
13. Schelkunoff, S. A. . . . . *I.R.E. Trans* , 1959, AP-7, S133.
14. Barlow, H. M. and Brown, J. . . Clarendon Press. 1962.
15. Wait, J. R. . . . . *Advance in Radio Research*, Academic Press, 1964, **4**, 157.
16. Barlow, H. M. and Cullen, A. L. . . *Proc. I.E.E* , Part iii, 1953, **100**, 329.
17. Marcuvitz, N.; Goubau, G., *et al* . . *Proceedings of the Symposium of Modern Advances in Mycrowave, Techniques, Polytechnic Institute of Brooklyn*, 1954, 481.
18. Collin, R. E. . . . . *Field Theory of Guided Waves*, Mc.Graw-Hill Book Company, 1960.
19. Zucker, F. J. . . . . *Proceedings of the Symposium on Modern Advances in Microwave Techniques, Polytechnic Institute of Brooklyn*, 1954, 403.
20. Tamir, T. and Oliner, A. A. . . *Proc., I.E.E E.*, 1963, **110**, 310.
21. Goubau, G. . . . . *I.R.E., Trans* , AP-7, Special Supplement, 1959, 140.
22. Adler, R. B. . . . . *Proc I R.E.*, 1952, 40, 339.
23. Collin, R. E. . . . . *Field Theory of Guided Waves*, Mc.Graw Hill Book Company, 1960, 485.
24. Wait, J. R. . . . . *I.R.E. Trans*. Special Supplement 1959, AP-7, 154.
25. Walkinshaw, W. . . . . *Proc. Phys. Soc.*, 1948, **61**, 246.

26	Hurd, R. A.	*Canadian J. of Phys* , 1954. **32**, 737.
27	Rotman, W.	*Proc. I R.E.*, 1951, **39**, 952.
28.	Piefke, G	*I.R.E., Trans.* AP-7, Special Supplement, 1959, 183.
29.	Chu, E. L. and Hansen, W. W. . .	*J. Appl. Phys.*, 1947, **18**, 996.
30.	Barlow, H. M. and Karbowiak, A.E.	*Proc. I.E.E* , Part iii, 1954, **101**, 182.
31.	Lines, A. W , Nicoll, G R. and Woodward, A M. . .	*Ibid*, 1950, **97**, 263.
32.	Harvey, A. F.	*I.R.E. Trans.* MTT-8, 1960, 30.
33.	Zacharia, K. P. and Chatterjee. S K.	*Proc I.E.R.E.*, (London), 1968, **36**, 111.
34.	Chatterjee, S. K. and Madhavan, P. . .	*J. Indian Institute of Science*, 1955 37, 200
35.	Chatterjee, S. K., Maskara and R. Chatterlee. .	*Proc. I E R.E.*, (Indian Division), 1968, **6**, 53.
36	Atwood, S S.	*J. Appl. Phys.* 1951, **22**, 504.
37.	Barlow, H. M. and Karbowiak, A. E.	*Proc. I.E E* , Part iii, 1953, **100**, 321.
38.	Roberts, T. E., ...	*J. Appl. phys.*, 1953, **24**, 57.
39.	Buchholz, H. . . .	*Annalen der physik, Leipzig*, 1940, **37**, 173.
40.	Froberg, C. E., ...	*Introduction to Numerical Analysis Addision* Wesley Publishing Company, Inc., Reading Massachusetts, Palo Alto, London, 1965.
41.	Kizner, W.	*J. Soc. Indust. Appl. Math* . 1964. **12**, 424.
42.	Contractor, S. N. and Chatterjee, S. K. . .	*J. Ind. Inst. of Science*, 1957, **39**, 67.
43.	Cullen, A. L. . . .	*Proc. I.E.E.*, Part iv, 1954, **101**, 225.
44.	Brown J. and Stachera, H. S. . .	*Ibid*, 106, Part B, Supplement. 1959, **13**, 143.
45.	Goubau, G.	*Proc. I.R.E.*, 1952, **40**, 865.
46.	Dyott, R. B.	*Proc. I.E.E.*, Part iii, 1952, **99**, 408.
47.	Duhamel. R. H. and Duncan, J. W.	*I R.E., Trans., MTT*-6, 1958, 277
48.	Wenger, N. C.	*I E.E E., Trans.*, 1965, AP-13, 126.
49.	Wait, J. R.	*J of Res. of the Nat. Bureau of Staddards*, 1959, **59**, 365
50.	(Miss.) H. M. Girija, Chatterjee S. K. . .	*J. Indian Institute of Science*, under publication